# CHAPTER 5: IDENTIFICATION OF GENETIC MODIFIER LOCI AT THE MOLECULAR LEVEL

## 5.1 INTRODUCTION

### 5.1.1 IDENTIFICATION OF INTERACTING REGIONS

Screening of the *Drosophila* genome using the Deficiency Kit (section 4.2.2) allowed the identification of numerous regions of the genome capable of modulating the GMR>DRAD21$^{DM}$ phenotype. Each region identified is therefore likely to contain candidate regulators of chromosome segregation or genes that can alter the GMR>DRAD21$^{DM}$ by some other mechanism. It is important at this point to keep in mind the possibility that some of the interactions may not be due to a direct affect on chromosome segregation, as demonstrated by the results of the GMRhid screen. The GMRhid screen identified seven enhancer regions and two suppressor regions that appear to contain modifiers acting via apoptosis. This indicated that enhancer interactions are less likely to be acting directly via the chromosome segregation pathway. As observed in previously published genetic screens numerous factors may act to make a process worse, and therefore enhance a phenotype. However, it is much more likely that improvement of a process occurs through suppression by acting directly on that process itself. For this reason, genomic regions capable of suppressing the GMR>DRAD21$^{DM}$ phenotype were focussed on.

The genome-wide screen and second-pass screening identified 48 genomic regions capable of modifying the GMR>DRAD21$^{DM}$ eye phenotype by mechanisms other than by apoptosis. Whilst the phenotypic effects observed were the result of deleting a large number of genes within each genomic region, the frequency of interacting deficiencies (62 out of 232) is strongly indicative that in most cases each deficiency will harbour a single DRAD21$^{DM}$ interacting locus.

In this chapter, 10 interacting genomic regions were examined in finer detail in order to identify as many of the causative loci at the molecular level as possible. This process and the results obtained are presented in this chapter. In addition, a mechanism of interaction is postulated for each of the identified interacting loci. In total 10 suppressors and 3 enhancers of GMR>DRAD21$^{DM}$ were unambiguously identified.

## 5.2 RESULTS

### 5.2.1 OVERVIEW

Figure 5.1 summarises the approaches used in this part of the study. A multi-pronged approach was employed to narrow down the chromosomal regions responsible for the phenotypic modifications with the aim of identifying as many causative loci at the molecular level as possible. Overlapping deletions were first used, where possible, to narrow down the size of the interacting region. Candidate genes were then identified within each interacting region and, where mutant alleles of these loci were available these were obtained and tested to see if they were capable of recapitulating the modification of the GMR>DRAD21$^{DM}$ eye phenotype.

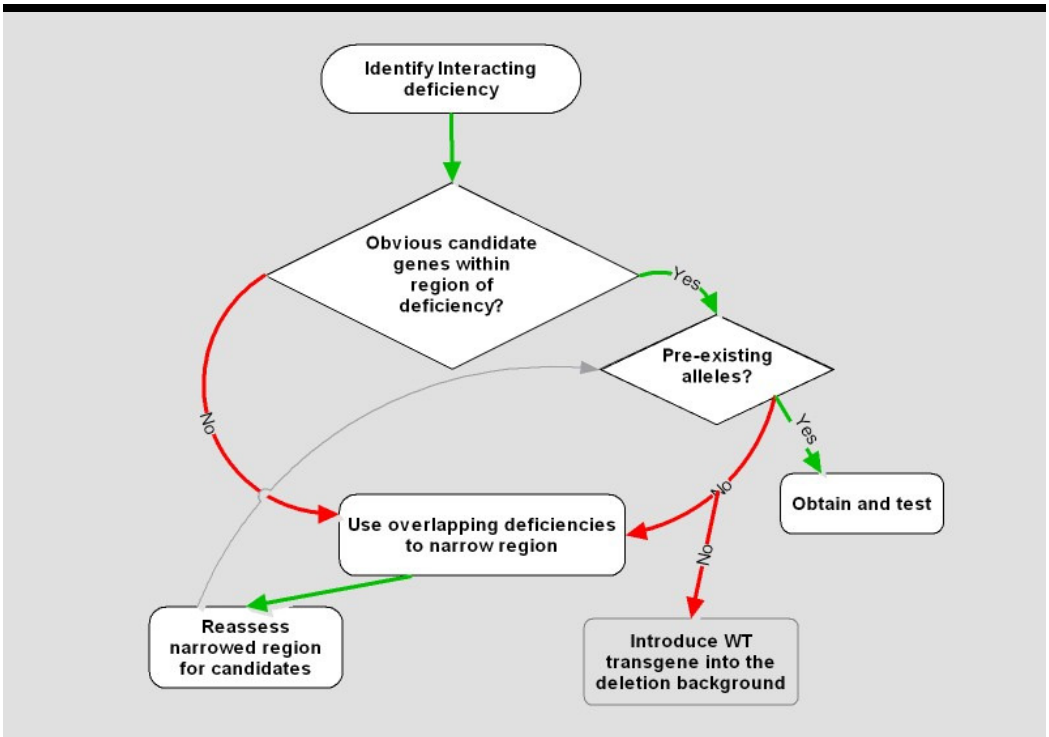


**Figure 5. 1:** *Flow chart of the approaches used to identify GMR>DRAD21$^{DM}$ interacting loci*

Note that the step of introducing the wild-type transgene into the deletion background to confirm the identity of the modifier gene when alleles were unavailable was not undertaken due to time constraints.

### 5.2.2 IDENTIFICATION OF *CyclinA* AS THE SUPPRESSOR LOCUS IN REGION S122

#### 5.2.2.1 S122 region overview

The S122 interaction belongs to the "Weak 1 Suppressor" phenotypic category (section 4.2.3.2). This phenotype is characterised by a mild suppression of the size defect and a moderate to strong suppression of the organisation defect of the GMR>DRAD21$^{DM}$ eye phenotype (Figure 4.9, Table 4.5).

The deficiency responsible for S122 (Df(3L)vin7) was obtained from BL stock 2612. This deficiency is on the left arm of the third chromosome and spans the polytene regions 68C8-11;69B4-5 deleting a minimum of 30 and maximum of 34 polytene bands. Analysis of the annotations of the 143-153 genes mapped to this region indicate that there are three genes encoding micro-RNAs, at least 25 genes encoding metabolic enzymes and at least six genes known to have roles in transcriptional regulation (Drysdale et al., 2005). A minimum of 54 genes within this region have an unknown function, being known only by their genome project (CG) number. Only 47 genes within this region have publicly available alleles. Genes known to be involved in regulating the cell cycle stood out as obvious candidates within this region, including the mitotic cyclin, *Cyclin A*. *Cyclin A* is known to be involved in the regulation of the $G_2$/M transition and CYC-A destruction facilitates chromosome disjunction (Parry and O'Farrell, 2001). *Cyclin A* therefore emerged as the prime candidate suppressor locus within this region.

### 5.2.2.2 Genetic dissection of region S122

In order to determine which of the 140 plus genes in region S122 was responsible for the genetic interaction observed, additional overlapping deletion lines hoped to enable refinement of the region of interaction were obtained. The first of these, Df(3L)vin3 (breakpoints 068C05-06;068E03-04) suppressed the GMR>DRAD21$^{DM}$ phenotype to a similar extent as the S122 phenotype (data not shown). An additional two deletions tested failed to modify the GMR>DRAD21$^{DM}$ phenotype (Figure 5.3). Taken together these data refined the region of interest down to the 68E1-4 interval (Figure 5.3). This region contains *Cyclin A*, which has been cytologically mapped to 68E1, further implicating it as the causative gene.

In order to determine if the S122 suppression was primarily due to deletion of *Cyclin A*, two mutant *CycA* alleles, *CycA*$^{C8LR1}$ and *CycA*$^{03946}$, were obtained and crossed into the GMR>DRAD21$^{DM}$ background. Both *CycA* alleles tested were capable of suppressing the reduced and roughened GMR>DRAD21$^{DM}$ eye phenotype, albeit to different extents (Figure 5.2). These data strongly support *CyclinA* as the S122 suppressor.

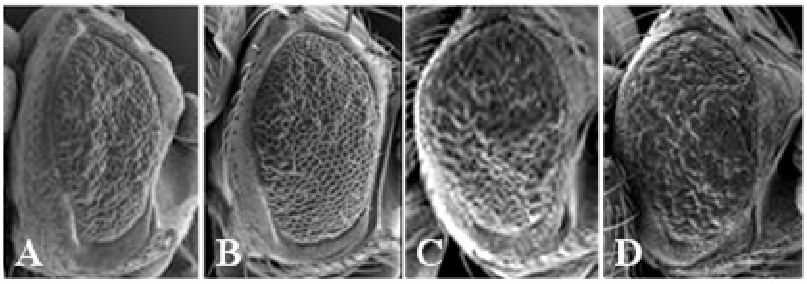


**Figure 5. 2:** *Mutations in Cyclin A suppress the GMR>DRAD21$^{DM}$ eye phenotype*

Scanning electron micrographs of adult *Drosophila* eyes, dorsal side is up and anterior to the right. **A:** The reduced and roughened eye phenotype of GMR>DRAD21$^{DM}$. **B:** The size and organisation defects of the GMR>DRAD21$^{DM}$ phenotype can be suppressed by the introduction of Df(3L)vin7 (S122)
**C** and **D:** The *Cyclin A* mutations, *CycA*$^{C8LR1}$ and *CycA*$^{03946}$, respectively, strongly suppress the GMR>DRAD21$^{DM}$ size defect, and minimally suppress the organisation defect.

**A.**

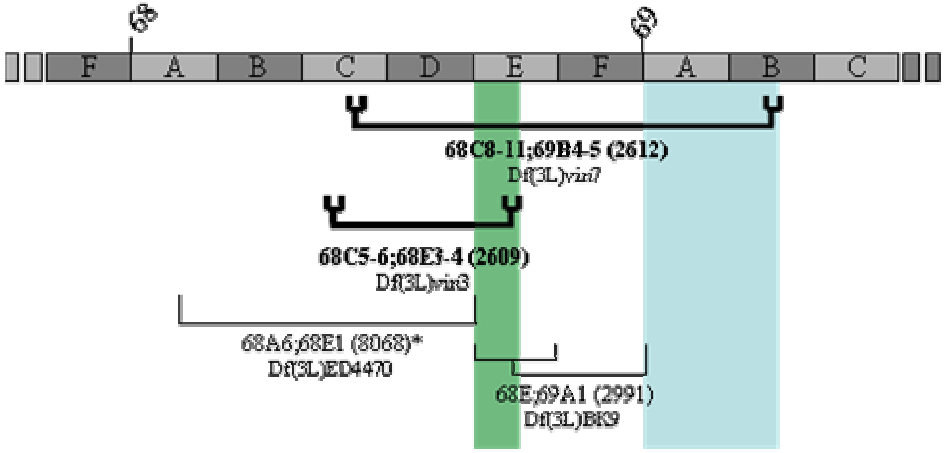
F
A
B
C
D
E
F
A
B
C
68C8-11;69B4-5 (2612)
Df(3L)vin7
68C5-6;68E3-4 (2609)
Df(3L)vin3
68A6;68E1 (8068)*
Df(3L)ED4470
68E;69A1 (2991)
Df(3L)BK9

**B.**

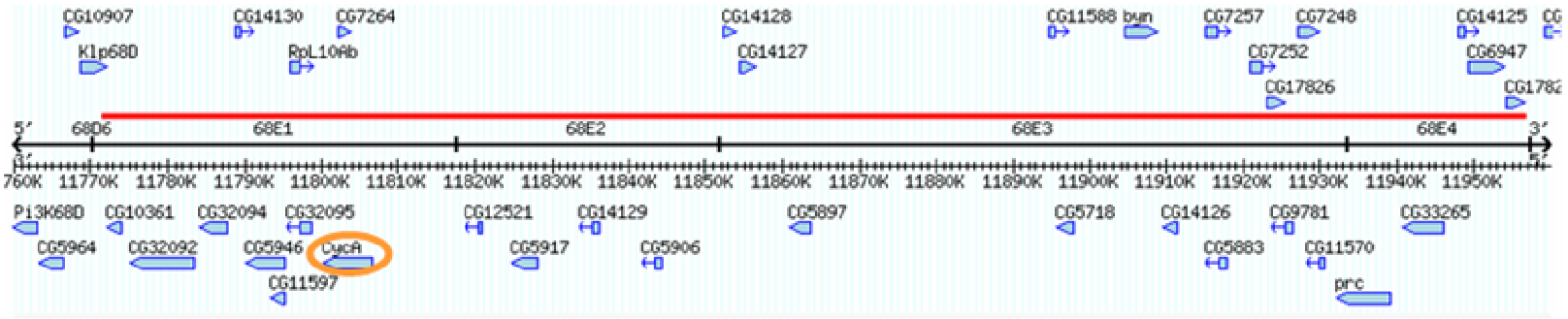
CG10907
CG14130
CG7264
CG14128
CG11588
bun
CG7257
CG7248
CG14125
Klp68D
RpL10Ab
CG14127
CG7252
CG6947
CG17826
5′
68D6
68E1
68E2
68E3
68E4
3′
760K
11770K
11780K
11790K
11800K
11810K
11820K
11830K
11840K
11850K
11860K
11870K
11880K
11890K
11900K
11910K
11920K
11930K
11940K
11950K
P13K68D
CG10361
CG32094
CG32095
CG12521
CG14129
CG5897
CG5718
CG14126
CG9781
CG33265
CG5964
CG32092
CG5946
CycA
CG5917
CG5906
CG5883
CG11570
CG11597
prc

**Figure 5. 3:** *Schematic of the region responsible for the S122 interaction*

**A:** Polytene divisions 68 and 69 of chromosome 3L are indicated and sub-divisions within each are shown. The deletion responsible for the S122 interaction is positioned closest to the chromosome schematic. Deletions that suppress the GMR>DRAD21$^{DM}$ eye phenotype are indicated in thick lines. Deletions that do not modify the GMR>DRAD21$^{DM}$ eye phenotype are also indicated in thin lines. Breakpoints and deficiency names are shown under each deletion, and BL stock numbers in brackets (Appendices 1 and 2). Breakpoints are mapped cytologically and in many cases are estimates only. Two regions that may contain suppressor loci are indicated as green and blue blocks. The region represented by the green block is shown in more detail in B.
**B:** Molecular map of the region putatively containing the suppressor locus (red line, green block in A). Numerous genes are contained within this small region, including the prime candidate suppressor *Cyclin A* (circled in yellow). Gene names are indicated. Also shown is a cytological map and molecular coordinates within chromosome 3L.
* the breakpoints of this deletion are estimated from release 3 of the *Drosophila* genome (Drysdale et al., 2005).

### 5.2.2.3 Proposed mechanism of suppression

The temporal co-ordination of mitotic events is determined by the degradation of the three mitotic cyclins, CYCLIN A, CYCLIN B and CYCLIN B3 (for review see Parry and O'Farrell, 2001). Overexpression of non-degradable forms of these proteins have shown that degradation of CYCLIN A is essential for chromosome segregation, degradation of CYCLIN B is required for anaphase and cytokinesis and destruction of CYCLIN B3 is required for re-organisation of the mitotic spindle and to establish an interphase nucleus (Parry and O'Farrell, 2001). These data highlight the distinct functions of each of the mitotic cyclins in mitotic progression.

In *Drosophila* it is the CYCLIN-A/CDC2 complex that performs the function of the mitosis promoting factor (MPF), since of the three mitotic cyclins, CYCLIN A is the only one essential for mitosis to occur (Dienemann and Sprenger, 2004, Jacobs et al., 2001). In the absence of CYCLIN A the substrates required for mitotic entry are degraded due to premature activation of the APC/C (Dienemann and Sprenger, 2004). The timing of the metaphase to anaphase transition is thought to be set by the co-operative actions of CYCLIN A, PIM (SECURIN) and the Cdk inhibitor, RUX (Su, 2001). This scenario implies a direct link between CYCLIN A and cohesin.

The suppression of the GMR>DRAD21$^{DM}$ eye phenotype observed upon halving the dose of *cycA* may be a result of incomplete inhibition of the APC/C. If this is the case

it follows that the levels of APC/C targets such as CYCLIN B and PIM (SECURIN) would be reduced. If the *cycA*-mediated suppression is due to the partial activation of the APC/C, a similar suppression phenotype should be observed by decreasing the levels of CYCLIN B in the GMR>DRAD21$^{DM}$ background. In testing whether the GMR>DRAD21$^{DM}$ phenotype was suitable for a genetic screen (Chapter 4, Table 4.1) the *CycB*$^{2}$ loss-of-function allele was shown to be a moderate-strong suppressor of the GMR>DRAD21$^{DM}$ organisation defect whilst only weakly suppressing the size defect (Figure 5.4). These results support the hypothesis that *cycA* mediated suppression is occurring through the partial activation of the APC/C. The phenotypes observed upon halving the dose of *cycA* and *cycB* are not identical (compare Figures 5.3 and 5.4). This difference may be due to the fact that partial activation of the APC/C due to reduced levels of functional CYCLINA/CDC2 will not only decrease the levels CYCLIN B but also of other APC/C targets such as PIM (SECURIN) and other anaphase inhibitory proteins. The suppression observed upon halving the dose of *cycA,* therefore, would be more likely due to the combined effects of partial reduction of numerous APC/C targets.

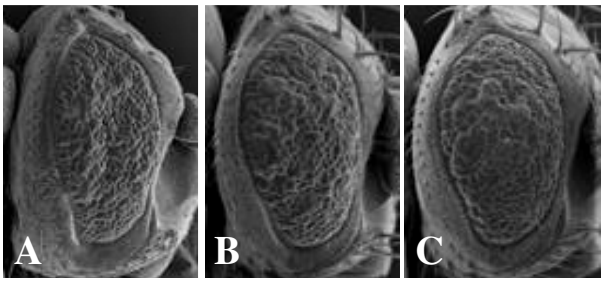


**Figure 5. 4:** *Mutations in Cyclin B suppress the GMR>DRAD21$^{DM}$ eye phenotype*

Scanning electron micrographs of adult *Drosophila* eyes, dorsal side is up and anterior to the right. **A:** The reduced and roughened eye phenotype of GMR>DRAD21$^{DM}$. **B** and **C:** Two examples of the suppression of the size and organisation defects of the GMR>DRAD21$^{DM}$ phenotype mediated by the introduction of the *cycB*$^{2}$ loss-of-function mutation.

### 5.2.3 IDENTIFICATION OF *eIF-4A* AS THE SUPPRESSOR LOCUS IN REGION S107

#### 5.2.3.1 S107 region overview

The S107 interaction belongs to the "Mixed Suppressor" phenotypic category (section 4.2.3.2). This phenotype is characterised by a moderate suppression of the GMR>DRAD21$^{DM}$ size and organisation defects, plus an additional distinct overgrowth phenotype (Figure 4.8, Table 4.5).

The deficiency responsible for S107 (Df(2L)BSC5) was obtained from BL stock 6299. This relatively small deficiency is on the left arm of the second chromosome and spans the polytene regions 26B1-2;26D1-2 deleting a minimum of 14 and maximum of 16 polytene bands. Analysis of the annotations of the 63 genes mapped to this region indicate that there are four genes encoding proteins involved in proteolysis, at least 5 genes encoding protein kinases and at least five genes known to have roles in transcriptional regulation (Drysdale et al., 2005). A minimum of 28 genes within this region have an unknown function and are known only by their genome project (CG) number. Only 24 genes within this region have publicly available alleles.

*lid*, *eIF4a*, and *Su(var)25F26B* were identified as possible candidate suppressor loci. *little imaginal discs (lid)*, maps to 26B2 and is a transcription factor involved in development known to interact genetically with the S-phase cyclin, *Cyclin E*, the epigenetic transcriptional regulator *ash1* and the chromatin remodelling factor *brahma* (Brumby et al., 2002, Gildea et al., 2000). *Su(var)25F26B* maps to 26B2-C1 and is involved in telomere silencing and position effect variegation (Mason et al., 2004, Wustmann et al., 1989, Reuter and Szidonya, 1983). *eIF4a* encodes a eukaryotic translation initiation factor located at 26B2 and is thought to regulate the translation of a specific set of cell cycle regulatory genes (Galloni and Edgar, 1999). *eIF4a* expression is upregulated in over-proliferation mutants (Hernandez et al., 2004) and e*IF4a* genetically interacts with the *Pten* tumour suppressor and S-phase regulators *Dp* and *E2F* (Galloni and Edgar, 1999).

#### 5.2.3.2 Genetic dissection of S107

In order to determine which of the 140 plus genes in this region was responsible for the interaction an additional deletion line that would refine the region of interaction was obtained. This deletion, Df(2L)AP1, has the breakpoints 26A;26B5-6 and was found to also suppress the GMR>DRAD21$^{DM}$ phenotype to the same extent as the S107 interaction. This allowed the refinement of the interacting region from 26B1-2;26D1-2 down to the 26B1-2;26B5-6 interval (Figure 5.5). This region potentially contains all three candidate genes discussed above, supporting their initial classification as candidate suppressor loci.

Of the three candidate suppressor genes, *Su(var)25F26B* does not have any publicly available mutant alleles and therefore could not be tested directly. It is also possible that *Su(var)25F26B* does not map to the suppressor region as its location remains imprecisely defined as spanning polytene bands 26B2-C1. Alleles of the remaining two candidates were obtained and crossed into the GMR>DRAD21$^{DM}$ background. The *lid* insertion allele, *lid*$^{10424}$, did not significantly alter the small and rough eye phenotype of GMR>DRAD21$^{DM}$. In contrast, both of the *eIF-4a* insertion alleles tested (*eIF4-a*$^{k01501}$ and *eIF-4a*$^{02439}$) were capable of suppressing the reduced and roughened eye phenotype to a similar extent as the original interacting deficiency (Df(2L)0BSC5) (Figure 5.6). This identifies *eIF-4a* as the primary locus responsible for the S107 interaction.

**A.**

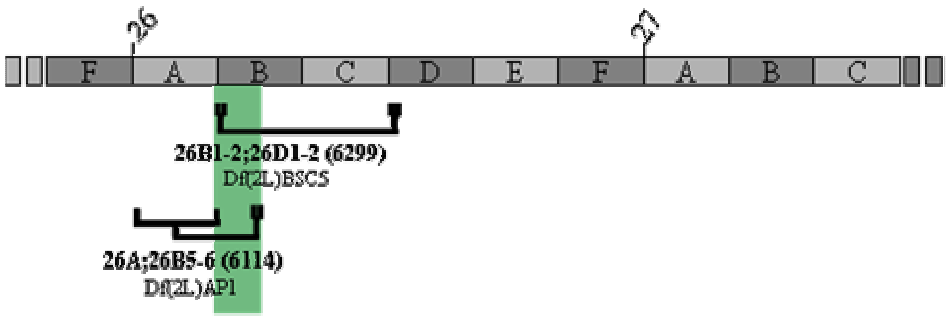
26
27
F
A
B
C
D
E
F
A
B
C
26B1-2;26D1-2 (6299)
Df(2L)BSC5
26A;26B5-6 (6114)
Df(2L)AP1

**B.**

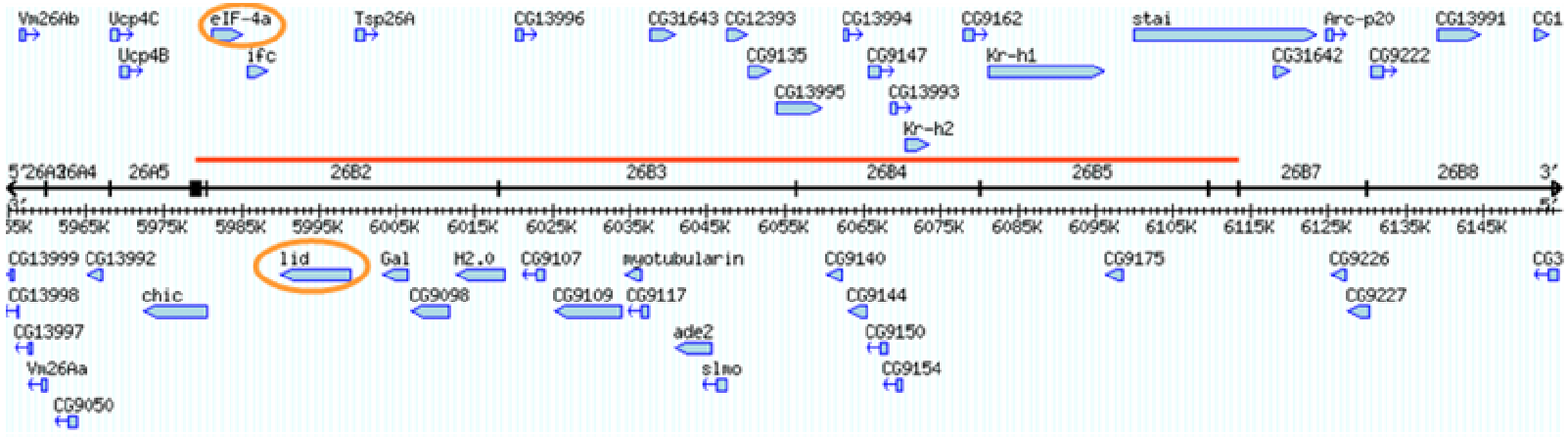
Vm26Ab
Ucp4C
eIF-4a
Tsp26A
CG13996
CG31643
CG12393
CG13994
CG9162
stai
Arc-p20
CG13991
Ucp4B
ifc
CG9135
CG9147
Kr-h1
CG31642
CG9222
CG13995
CG13993
Kr-h2
26A5
26B2
26B3
26B4
26B5
26B7
26B8
CG13999
CG13992
lid
Gal
H2.0
CG9107
myotubularin
CG9140
CG9175
CG9226
CG13998
chic
CG9098
CG9109
CG9117
CG9144
CG9227
CG13997
ade2
CG9150
Vm26Aa
slmo
CG9154
CG9050

**Figure 5. 5:** *Schematic of the region responsible for the S107 interaction*

**A:** Polytene divisions 26 and 27 of chromosome 2L are indicated and sub-divisions within are shown. The deletion responsible for the S107 interaction is positioned closest to the chromosome schematic. Deletions that suppress the GMR>DRAD21$^{DM}$ eye phenotype are indicated in thick lines. Breakpoints and deficiency names are shown under each deletion, and BL stock numbers in brackets. Breakpoints are mapped cytologically and in many cases are estimates only. The narrowed region likely to contain the suppressor locus/loci is indicated by the green block and is shown in more detail in B.
**B:** Molecular map of the region putatively containing the suppressor locus (red line, green block in A). Numerous genes are contained within this small region, including the candidate suppressors *eIF4A* and *lid* (circled in orange). The third candidate is not represented here, and its position has been mapped to within the region spanning 26B2-C1. Gene names are indicated. Also shown is a cytological map and molecular coordinates within chromosome 2L.

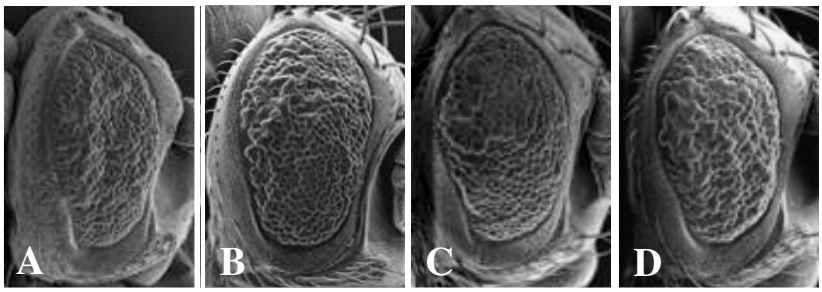


**Figure 5. 6:** *Mutations in eIF-4a suppress the GMR>DRAD21$^{DM}$ eye phenotype*

Scanning electron micrographs of adult *Drosophila* eyes, dorsal side is up and anterior to the right. **A:** The reduced and roughened eye phenotype of GMR>DRAD21$^{DM}$. **B:** The size and organisation defects of the GMR>DRAD21$^{DM}$ phenotype are moderately suppressed by the introduction of Df(2L)BSC5 (S107). **C** and **D:** The *eIF-4a* mutations *eIF-4a$^{02439}$* and *eIF-4a$^{k01501}$*, respectively, can moderately suppress the GMR>DRAD21$^{DM}$ size and organisation defects.

#### 5.2.2.3 Proposed mechanism of suppression

The mechanism by which mutations in a translation initiation factor such as *eIF4a* may mediate suppression of the GMR>DRAD21$^{DM}$ eye phenotype was not immediately obvious. *eIF4a* encodes a DEAD-box RNA helicase that functions as a eukaryotic translation initiation factor, thought to regulate the translation of a specific set of cell cycle regulatory genes (Galloni and Edgar, 1999). *Drosophila eIF4a* expression is upregulated in over-proliferation mutants (Hernandez et al., 2004) and e*IF4a* genetically interacts with the *Pten* tumour suppressor and S-phase regulators *Dp* and *E2F* (Galloni and Edgar, 1999). *eIF4a* is essential for cell growth and acts as a dose-dependent growth regulator (Galloni and Edgar, 1999, Gao et al., 2000, Linder and Slonimski, 1989). Metaphase entry is slow in *eIF4a* mutants of *S.pombe* due to inefficient translation of required proteins including Cdc25 (Linder and Slonimski, 1989), supporting the proposition that eIF-4A is required for the translation of a subset of cell cycle regulatory genes. eIF-4A target transcripts have not been studied in *Drosophila*, however, target conservation could aid in explaining the suppression observed in this study.

CDC25/STRING is required to activate the CDC2 mitotic cyclin partner and therefore promote mitotic entry. If CDC25/STRING translation is inefficient in *Drosophila eIF4a* mutants, mitotic entry would be delayed due to a decrease in the level of activated CYCLIN/CDC2 complexes. Consistent with this, halving the genetic dose of both *cycA* and *cycB* also suppress the GMR>DRAD21$^{DM}$ eye phenotype. It is hypothesised that *eIF4a* mediated suppression of the GMR>DRAD21$^{DM}$ eye phenotype observed in this study is a direct result of the impaired translation of cell cycle regulatory genes such as *Cdc25/string*. The contribution of reduced CDC25/STRING and CDC2 function to the observed phenotype could be tested directly by obtaining mutant alleles for each of these genes and crossing them into the GMR>DRAD21$^{DM}$ background, however time did not allow this further analysis.

### 5.2.4 IDENTIFICATION OF *HDAC4* AS THE SUPPRESSOR LOCUS IN REGION S79

#### 5.2.4.1 S79 region overview

The S79 interaction belongs to the "Weak 3 Suppressor" phenotypic category (Section 4.2.3.2). This phenotype is characterised by a weak-moderate suppression of the GMR>DRAD21$^{DM}$ size and organisation defects, plus a distinct increase in the number of bristle cells in the eye (Figure 4.9, Table 4.5).

The deficiency responsible for S79 (Df(1)N12) was obtained from BL stock 966. This relatively small deficiency is on the X chromosome and spans the polytene regions 11D1-2;11F1-2 deleting a minimum of 23 and maximum of 25 polytene bands. Analysis of the annotations of the 71 genes mapped to this region indicate that there are three genes encoding proteins involved signalling and at least three genes encoding protein kinases (Drysdale et al., 2005). A minimum of 32 genes within this region have an unknown function and are known only by the number assigned to them by the genome project (CG number). Only 22 genes within this region have publicly available alleles.

#### 5.2.4.2 Genetic dissection of region S79

The Deficiency Kit deletions Df(1)JA26 (BL stock 964) and Df(1)C246 (BL stock 967) have break points that overlap with those of the deficiency responsible for the S79 interaction (Df(1)N12). The Df(1)JA26 deletion enhances the GMR>DRAD21$^{DM}$ phenotype and is responsible for the E126 moderate enhancement interaction (not investigated further), while Df(1)C246 does not modify the phenotype. The breakpoints of these two additional deletions, although imprecisely defined, aid in narrowing the region of interaction from 11D1-2;11F1-2 down to the 11D1;11E12 interval (Figure 5.7). Analysis of the annotations of the 62 genes within the narrowed region identified a total of six obvious candidate genes: *hep, lic, Bap60, sno, comt,* and *HDAC4*.

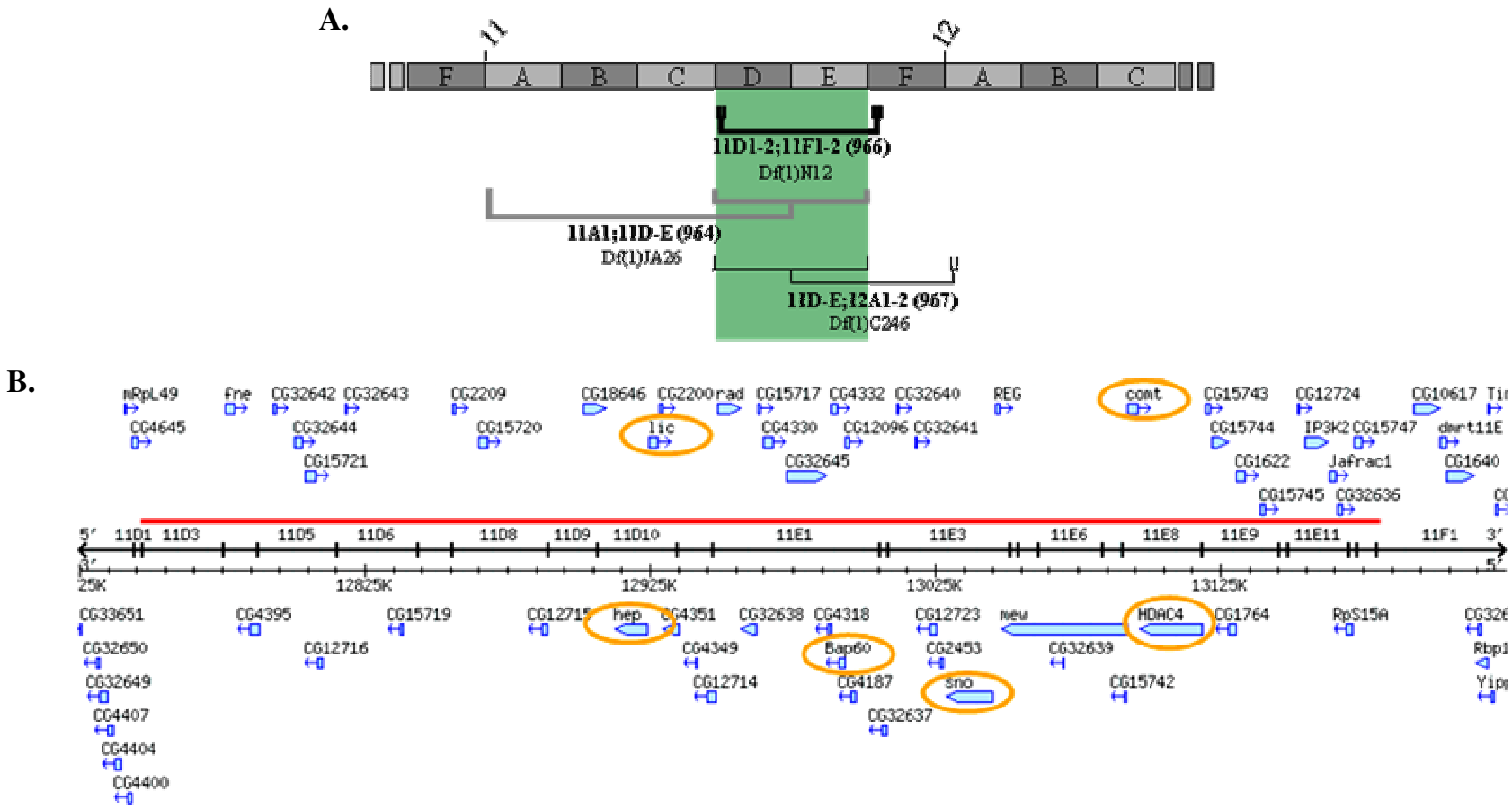
A.
11
12
F
A
B
C
D
E
F
A
B
C
11D1-2;11F1-2 (966)
Df(1)N12
11A1;11D-E (964)
Df(1)JA26
11D-E;12A1-2 (967)
Df(1)C246
B.
nRpL49
fne
CG32642
CG32643
CG2209
CG18646
CG2200
rad
CG15717
CG4332
CG32640
REG
comt
CG15743
CG12724
CG10617
CG4645
CG32644
CG15720
lic
CG4330
CG12096
CG32641
CG15744
IP3K2
CG15747
dwrt11E
CG15721
CG32645
CG1622
Jafrac1
CG1640
CG15745
CG32636
5'
11D1
11D3
11D5
11D6
11D8
11D9
11D10
11E1
11E3
11E6
11E8
11E9
11E11
11F1
3'
25K
12825K
12925K
13025K
13125K
CG33651
CG4395
CG15719
CG12715
hep
CG4351
CG32638
CG4318
CG12723
neu
HDAC4
CG1764
RpS15A
CG32650
CG12716
CG4349
Bap60
CG2453
CG32639
Rbp1
CG32649
CG12714
CG4187
sno
CG15742
CG4407
CG32637
CG4404
CG4400

**Figure 5. 7:** *Schematic of the region responsible for the S79 interaction*

**A:** Polytene divisions 11 and 12 of chromosome 1 (X) are indicated and sub-divisions within are shown. The deletion responsible for the S79 interaction is positioned closest to the chromosome schematic. Deletions that suppress the GMR>DRAD21$^{DM}$ eye phenotype are indicated by thick black lines, those that enhance the phenotype are indicated by thick grey lines. Deficiencies that do not modify the GMR>DRAD21$^{DM}$ phenotype are indicated by thin black lines. Breakpoints and deficiency names are shown under each deletion, and BL stock number in brackets. Breakpoints are mapped cytologically and in many cases are estimates only. The narrowed region likely to contain the suppressor locus/loci is indicated by the green block and is shown in more detail in B.
**B:** Molecular map of the region putatively containing the suppressor locus (red line, green block in A). Numerous genes are contained within this small region, including the candidate suppressors *hep, lic, Bap60, sno, comt* and *HDAC4* (circled in orange). Gene names are indicated. Also shown is a cytological map and molecular coordinates within chromosome 1.

The contribution of candidate suppressor loci *Bap60* and *comt,* to the S81 interaction was unable to be tested due to the lack of publicly available alleles. *Brahma associated factor of 60kDa* (*Bap60*), is involved in chromatin remodelling, and *comt*, is predicted to have mitotic roles (Drysdale et al., 2005). Alleles that were tested directly included *hep$^{r75}$*, *hep$^{G0107}$*, *lic$^{G0252}$*, *sno$^{KG10357}$*and *HDAC4$^{KG09091}$*.

The *Drosophila* homologue of the mammalian mitogen activated kinase 7 (MAPK 7) *hemiopterous*, or *hep*, maps to 11D10. Genetic interactions with the *Src42A* oncogene, the Ras related protein *Rala* and Ras GTP-ase *Rac1* implicate *hep* in cell proliferation, cell cycle regulation and imaginal disc morphogenesis (Sawamoto et al., 1999, Tateno et al., 2000, Stronach and Perrimon, 2002, Fanto et al., 2000). To determine if the S97 interaction is due to the deletion of *hep* the *hep* alleles *hep$^{r75}$* and *hep$^{G0107}$* were crossed into the GMR>DRAD21$^{DM}$ background. Neither of the alleles tested suppressed the reduced and roughened eye phenotype of GMR>DRAD21$^{DM}$.

*licorne*, or *lic*, maps to 11D10 and encodes a MAPKK involved in the specification of cell fate. *lic* and its mammalian p38 kinase homologues have been implicated in a diverse range of processes including development, cell proliferation and cell survival (Nebreda and Porras, 2000). The insertion allele *lic$^{G0252}$* failed to modify the GMR>DRAD21$^{DM}$ phenotype, ruling-out *lic* as the causative locus for the S97 suppression.

*strawberry notch* (*sno*) located at 11E3 is a helicase involved in the Notch and epidermal growth factor signalling pathways. Genetic interactions with the Notch signal transducer *Delta*, cytoskeletal component *discs large 1* (*dgl1*) and the S-phase protein EBI implicate *sno* in cell fate commitment in the eye, and regulation of both cell proliferation and the cell cycle (Coyle-Thompson and Banerjee, 1993, Tsuda et al., 2002). The insertion allele $sno^{KG10357}$ did not modify the GMR>DRAD21$^{DM}$ phenotype, ruling *sno* out as the causative locus for the S97 suppression.

A sixth and final candidate suppressor locus identified in this region was that of *histone deacetylase 4* (*HDAC4*), located at 11E8. Transcription of *HDAC4* during embryogenesis is regulated by gap and pair rule genes (Marija Zeremski, 2003). *HDAC4* encodes a protein called HDAC4a with roles in segmentation and putative roles in DNA binding and histone modification. Yeast-two hybrid analysis shows that HDAC4a binds the adaptor protein 14-3-3zeta which is known to be involved in chromosome segregation and cell proliferation (Breitkreutz et al., 2003). This implicates *HDAC4* indirectly in chromosome segregation. The insertion allele $HDAC4^{KG09091}$ was obtained and shown to be capable of modifying the GMR>DRAD21$^{DM}$ phenotype to a similar extent as the original deficiency, increasing both the size and organisation of the eye (Figure 5.8). This identifies *HDAC4* as the primary locus responsible for the S79 interaction.

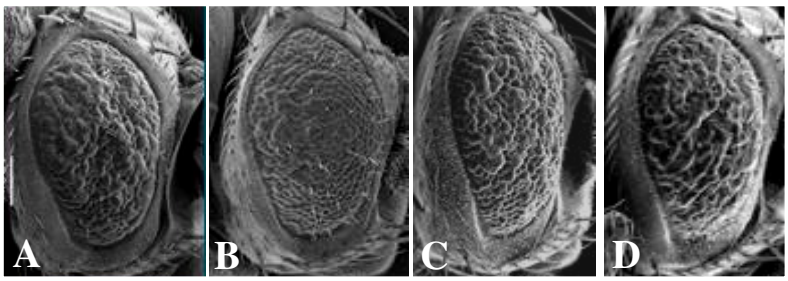


**Figure 5. 8:** *Mutations in HDAC4 suppress the GMR>DRAD21DM eye phenotype*

Scanning electron micrographs of adult *Drosophila* eyes, dorsal side is up and anterior to the right. **A:** The reduced and roughened eye phenotype of GMR>DRAD21$^{DM}$. **B:** The size and organisation defects of the GMR>DRAD21$^{DM}$ phenotype are suppressed by the introduction of Df(1)N12 (S122) **C** and **D:** Two examples of $HDAC4^{KG09091}$ mediated suppression of the GMR>DRAD21$^{DM}$ eye phenotype. The *HDAC4* mutation $HDAC4^{KG09091}$ suppressed the size and organisation defects and also exhibits increased bristles.

#### 5.2.4.3 Proposed mechanism of suppression

The centromeric region of all eukaryotic chromosomes is characterised by a number of cytological features including the presence of heterochromatin. Mutations that interfere with the formation of heterochromatin result in defects in chromosome segregation, indicating that chromatin state is an important factor in the regulation of chromosome dynamics (Allshire et al., 1995, Ekwall et al., 1999, Hari et al., 2001, Kellum and Alberts, 1995, Walfridsson et al., 2005). Studies in fission yeast have shown that heterochromatin is required for the recruitment and/or stabilisation of cohesin at the centromere (Bernard and Allshire, 2002, Bernard et al., 2001b, Nonaka et al., 2002). In metazoan species it is the centromeric pool of cohesin that maintains cohesion between sister chromatids until the metaphase to anaphase transition, and it is likely that chromatin state is important in defining the different pools of cohesin in metazoan species. This supposition is supported by the fact that human RAD21 can bind the catalytic subunit of the ISWI chromatin remodelling complex, and that this association depends upon ISWI chromatin remodelling activity (Hakimi et al., 2002).

Histone hypoacetylation is a hallmark of silent chromatin, and halving the dose of *Drosophila HDAC4,* which encodes a histone deacetylase, is likely to affect the level of histone acetylation. Increased acetylation may result in a decrease in the amount of heterochromatin in the vicinity of the centromere and subsequently affect the level of cohesin loading. In fission yeast, histone deacetylation is important for the assembly of the silent HP1/SWI6 containing chromatin domains (for review see (Moazed, 2001). SWI6 has been shown to recruit and/or maintain centromeric cohesion in *S. pombe,* and the SCC3 homologue, PSC3, has been shown to bind SWI6 (Nonaka et al., 2002) indicating that SWI6 plays a direct role in the recruitment of cohesin to the centromere.

It is possible that *HDAC4* mediated suppression of the GMR>DRAD21$^{DM}$ phenotype is the result of decreased centromeric recruitment of cohesin, and therefore, a local reduction in the strength of cohesion. This hypothesis could be tested directly by comparing the distribution of cohesin on the chromosomes of wild-type and *HDAC4* mutants. However, time constraints did not allow for these analyses to be performed.

### 5.2.5 IDENTIFICATION OF *dup* AS THE SUPPRESSOR LOCUS IN REGION S67

#### 5.2.5.1 S67 region overview

The S67 interaction was placed in the "Strong Suppressor" phenotypic category (Section 4.2.3.2). This phenotype is characterised by an increase in both the size and the organisation of the GMR>DRAD21$^{DM}$ eye phenotype resulting in an almost wild-type appearance (Figure 4.8, Table 4.5).

The deficiency responsible for S67 (Df(2R)Jp1) was obtained from BL stock 3518. This deficiency is on the right arm of the second chromosome and spans the polytene regions 51D3-8;52F5-9, deleting a minimum of 90 and maximum of 97 polytene bands. Analysis of the annotations of the 134-150 genes mapped to this region indicate that there are eight genes encoding metabolic enzymes, at least seven genes encoding protein kinases and at least five genes known to have roles in proteolysis and peptidolysis (Drysdale et al., 2005). A minimum of 59 genes within this region have an unknown function being known only by their genome project (CG) number. Only 51 genes within this region have publicly available alleles.

#### 5.2.5.2 Genetic dissection of region S67

In order to determine which of the 130 plus genes in this region was responsible for the S67 interaction additional deletion lines that would refine the region of interaction were obtained. Deletions Df(2R)XTE-18 and Df(2R)XTE-11, with the breakpoints 51E3;52C9-D1 and 51D3-E4;52A6-10 respectively were observed to suppress the GMR>DRAD21$^{DM}$ phenotype to a similar extent as observed in S67. In addition, the Deficiency Kit deletion, Df(2R)Jp8, responsible for the E71 interaction, partially overlaps with the S67 deletion (Figure 5.9). The data from these overlapping deletions narrowed the interaction region from 51D3-8;52F2-9 to 51E3;52A6 (Figure 5.9). Analysis of the annotations of the 46 genes in this region revealed three obvious candidate genes likely to be responsible for the S67 phenotype.

**A.**

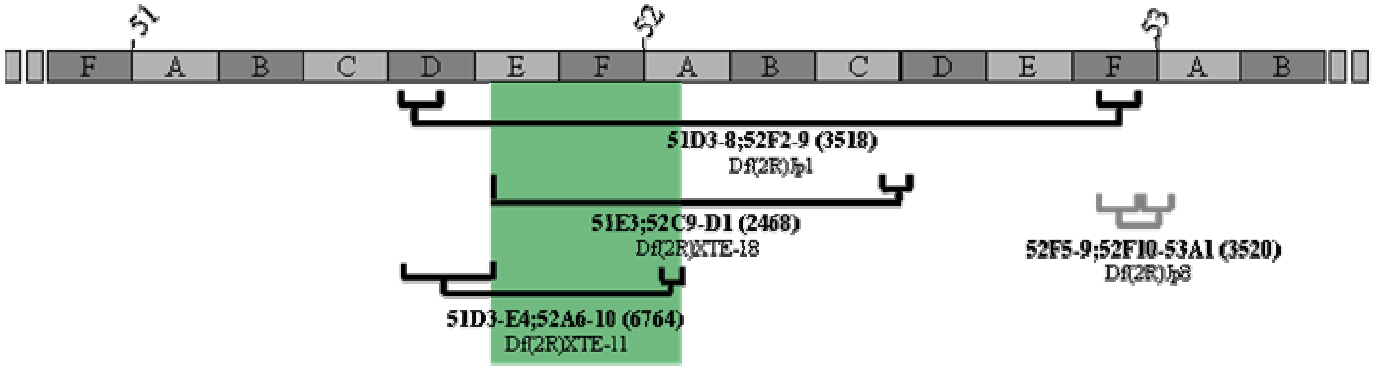
51
52
53
F A B C D E F A B C D E F A B
51D3-8;52F2-9 (3518)
Df(2R)Jp1
51E3;52C9-D1 (2468)
Df(2R)XTE-18
52F5-9;52F10-53A1 (3520)
Df(2R)Jp8
51D3-E4;52A6-10 (6764)
Df(2R)XTE-11

**B.**

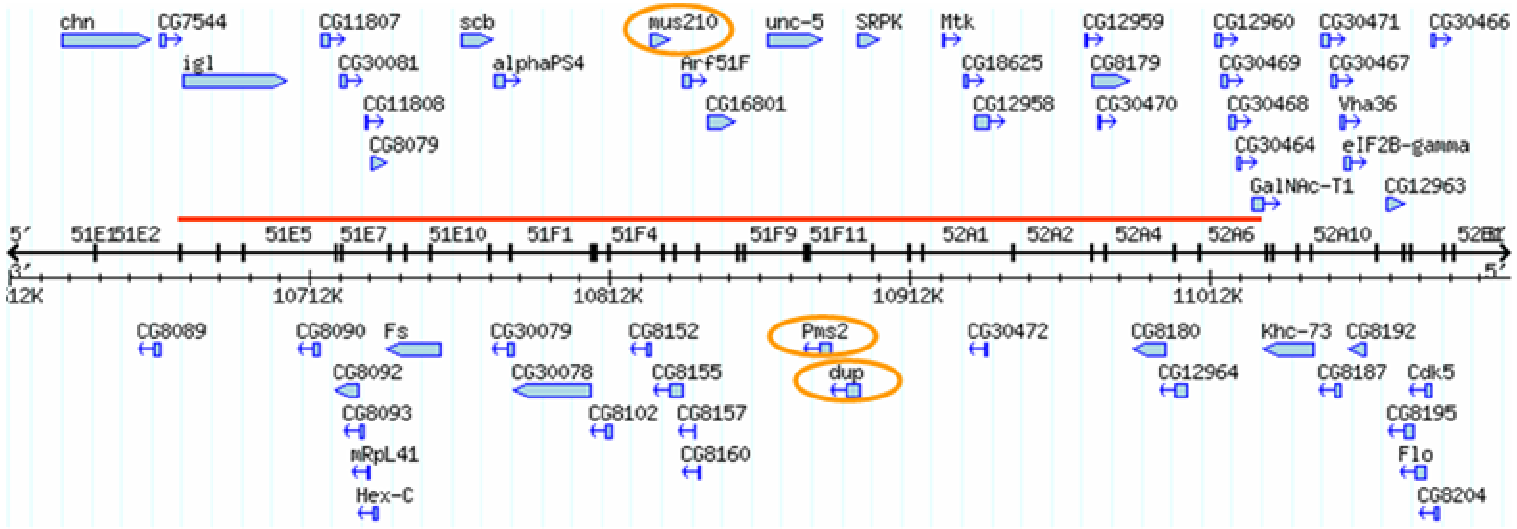
chn
CG7544
igl
CG11807
CG30081
CG11808
CG8079
scb
alphaPS4
mus210
Arf51F
CG16801
unc-5
SRPK
Mtk
CG18625
CG12958
CG12959
CG8179
CG30470
CG12960
CG30469
CG30468
CG30464
GalNAc-T1
CG30471
CG30467
Vha36
eIF2B-gamma
CG12963
CG30466
5′
51E1
51E2
51E5
51E7
51E10
51F1
51F4
51F9
51F11
52A1
52A2
52A4
52A6
52A10
3′
12K
10712K
10812K
10912K
11012K
CG8089
CG8090
Fs
CG8092
CG8093
mRpL41
Hex-C
CG30079
CG30078
CG8102
CG8152
CG8155
CG8157
CG8160
Pms2
dup
CG30472
CG8180
CG12964
Khc-73
CG8192
CG8187
Cdk5
CG8195
Flo
CG8204

**Figure 5. 9:** *Schematic of the region responsible for the S67 interaction*

**A:** Polytene divisions 51, 52 and 53 of chromosome 2R are indicated and sub-divisions within are shown. The deletion responsible for the S67 interaction is closest to the chromosome schematic. Deletions that suppress the GMR>DRAD21$^{DM}$ eye phenotype are indicated by thick black lines, those that enhance the phenotype are indicated by thick grey lines. A deletion that enhances the GMR>DRAD21$^{DM}$ phenotype (E71) is also shown. Breakpoints and deficiency names are shown under each deletion, and BL stock numbers in brackets. Breakpoints are mapped cytologically and in many cases are estimates only. The narrowed region likely to contain the suppressor locus/loci is indicated by the green block and is shown in more detail in B.
**B:** Molecular map of the region putatively containing the suppressor locus (red line corresponding to green block in A). Numerous genes are contained within this small region, including the candidate loci *mus210*, *Pms2* and *dup* (circled in orange). Gene names are indicated. Also shown is a cytological map and molecular coordinates within chromosome 2R.

Two of the candidate genes, *Pms2* and *mus210,* encode mismatch and nucleotide excision repair proteins respectively (Sekelsky et al., 2000, Henning et al., 1994). The integrity of DNA and DNA repair processes are crucial in the maintenance of genomic and chromosome stability, making both of these genes candidate suppressors. Unfortunately, in the absence of mutant alleles the contribution of these loci to the S67 phenotype was unable to be tested.

The third and final candidate suppressor locus identified in this region was that of *double parked* (*dup*) located at 51F11. DUP, the *Drosophila* Cdt1 homologue, is a DNA replication factor that forms part of the origin of recognition complex (ORC). Mutations in many ORC proteins, including DUP, cause defects in chromosome condensation and DNA replication (Whittaker et al., 2000, Christensen and Tye, 2003). DUP has been shown to physically interact with the DNA replication initiation factor GEMININ and genetically interact with the *Drosophila* DNA repair and spindle checkpoint factors *mei-41* (*ATM*) and *bub1* (Garner et al., 2001, Quinn et al., 2001). Recently its mammalian counterpart, Cdt1, has been identified as a potential oncogene (Arentson et al., 2002, Saxena and Dutta, 2005). In *Xenopus* recruitment of Scc2, the cohesin loading factor, and cohesin to chromatin is dependent on the ORC and Dup (Takahashi et al., 2004, Gillespie and Hirano, 2004). These factors make *dup* a prime candidate for modification of the GMR>DRAD21$^{DM}$ phenotype. To determine if *dup* was the causative locus for the S67 interaction four *dup* alleles were obtained and tested. All four were shown to modulate the GMR>DRAD21$^{DM}$ phenotype, primarily

by increasing the organisation of the eye, albeit to different extents (Figure 5.10). None of the *dup* alleles tested modified the GMR>DRAD21$^{DM}$ phenotype to the same extent as the original deficiency. These results indicate that the S67 interaction is due, at least in part, to the deletion of the *dup* gene, although the existence of other weak suppressor loci in the region cannot be ruled out.

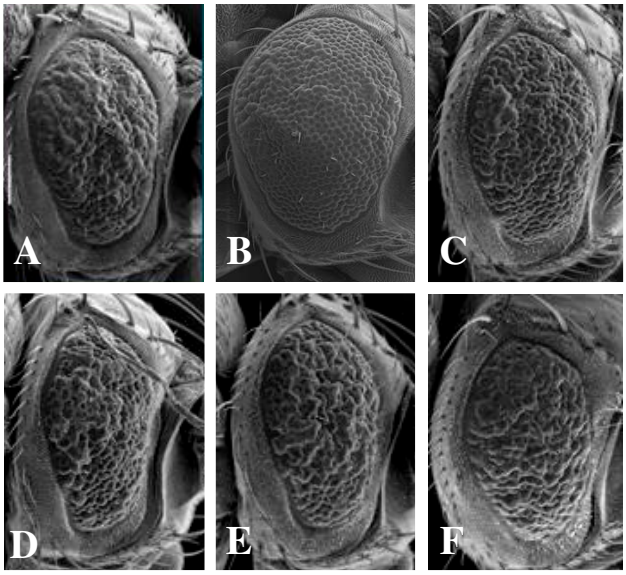


**Figure 5. 10:** *Mutations in Dup suppress the GMR>DRAD21$^{DM}$ eye phenotype*

Scanning electron micrographs of adult *Drosophila* eyes, dorsal side is up and anterior to the right. **A:** The reduced and roughened eye phenotype of GMR>DRAD21$^{DM}$. **B:** The GMR>DRAD21$^{DM}$ size and organisation defects are suppressed by the introduction of Df(2R)Jp1 (S67). **C-F:** *dup* mutations *dup$^{PA77}$* (**C**), *dup$^{K03308}$* (**D**), *dup$^{a3}$* (**E**) and *dup$^{a1}$* (**F**) increase the organisation of the GMR>DRAD21$^{DM}$ eye and also slightly increase the size, but not to the same extent as the S67 deficiency.

### 5.2.5.3 Proposed mechanism of suppression

In *Xenopus*, recruitment of the cohesin loading factor SCC2 to chromatin is dependent on CDT1/DUP and the origin recognition complex (Takahashi et al., 2004, Gillespie and Hirano, 2004). Halving the dose of *dup* is likely to be suppressing the GMR>DRAD21$^{DM}$ phenotype by globally reducing the loading of cohesin, at both chromosome arms and at centromeres. This contention is supported by the fact that halving the dose of *scc2/nippedB* also suppressed the GMR>DRAD21$^{DM}$ eye phenotype (Section 4.2.1).

The function of DUP is modulated by its inhibitory binding partner GEMININ, and it has been proposed that a balance between DUP and GEMININ is important for maintaining genomic stability (Saxena and Dutta, 2005). Overexpression of GEMININ in the GMR>DRAD21$^{DM}$ background should produce a suppression phenotype similar to that of halving the dose of *dup*, and therefore provide further evidence that DUP activity is required for chromosome segregation. Analysis of the distribution of cohesin proteins along both wild-type and *dup* mutants would establish whether cohesin loading is affected in *dup* mutants, and provide direct evidence for the conservation of cohesin loading in metazoan species.

### 5.2.6 IDENTIFICATION OF *Scim13* AS THE SUPPRESSOR LOCUS IN REGION S81

#### 5.2.6.1 S81 region overview

The S81 interaction belongs to the "Moderate-Strong" phenotypic category (Section 4.2.3.2). This phenotype is characterised by an increase in both the size and the organisation of the GMR>DRAD21$^{DM}$ eye phenotype resulting in substantially more wild-type appearance (Figure 4.8, Table 4.5).

The deficiency responsible for S81 (Df(2L)C144) and was obtained from BL stock 90. This deficiency is on the right arm of the second chromosome and spans the polytene regions 22F3-4;23C3-5 deleting a minimum of 19 and maximum of 22 polytene bands and 66-95 genes. Analysis of the annotations of the genes mapped to this region indicate that there are at least six genes encoding metabolic enzymes, at least five genes encoding transcription factors and at least four genes known to have roles in glycolysis (Drysdale et al., 2005). A minimum of 18 genes within this region have an unknown function and are known only by their genome project (CG) number. Only 31 genes within this region have publicly available alleles.

#### 5.2.6.2 Genetic dissection of region S81

Two other Deficiency Kit deletions have breakpoints that overlap with that of Df(2L)C144. The first of these, Df(2L)dpp$^{d14}$ does not modify the GMR>DRAD21$^{DM}$ phenotype, whilst the second of these, Df(2L)JS17, enhances the eye phenotype and is responsible for the E240 interaction (not investigated further). An additional deletion line, Df(2L)D20, was obtained to further refine the region of interaction. This deletion has the breakpoints 22F4;23A1 and does not modify the GMR>DRAD21$^{DM}$ phenotype. Taken together, the data from these three deletions narrowed the interacting region from cytological region 22F3-4;23C3-5 down to the 23A1;23C3-5 interval (Figure 5.11). This refined region of interaction deletes a minimum of 17 polytene bands, and at least 81 genes. A total of seven candidate genes were identified within this region (Figure 5.11), including two that were unable to be tested due to the lack of publicly available alleles. Alleles that were tested directly included *Drp1*$^{K03815}$, *Su(var)2-4*$^{01}$, *lilli*$^{k05431}$, *Scim12*$^{2}$ and *Scim13*$^{1}$.

The contribution of two identified candidate loci to the S81 interaction was unable to be tested due to the lack of publicly available alleles. Loci that were unable to be tested included the *rad1* DNA repair and cell cycle control gene (Lydall and Weinert, 1995, Onel et al., 1996, Thelen et al., 1999), and *p16-ARC* which encodes a protein involved in centrosome positioning and is a structural constituent of the cytoskeleton (Robinson et al., 2001, Welch et al., 1997).

The dynamin related protein, DRP1, is a GTPase and is a constituent of the cytoskeleton with roles in endocytosis. The related human protein MxB has recently been shown to be involved in cell cycle progression, presumably by controlling the rate of nuclear import (King et al., 2004). The *Drp1* insertion allele, *Drp1*$^{K03815}$, failed to suppress the GMR>DRAD21$^{DM}$ phenotype, ruling *Drp1* out as the causative gene for the S81 interaction.

**A.**

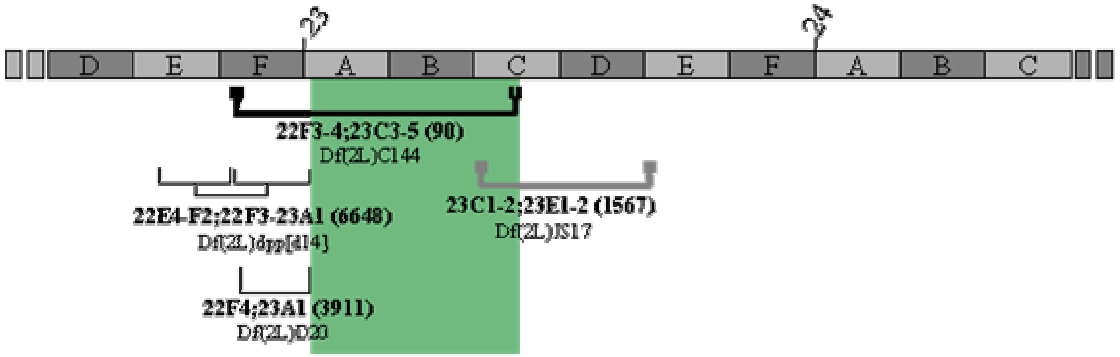
D E F A B C D E F A B C
22F3-4;23C3-5 (90)
Df(2L)C144
22E4-F2;22F3-23A1 (6648)
Df(2L)dpp[4l4]
23C1-2;23E1-2 (1567)
Df(2L)JS17
22F4;23A1 (3911)
Df(2L)D20

**B.**

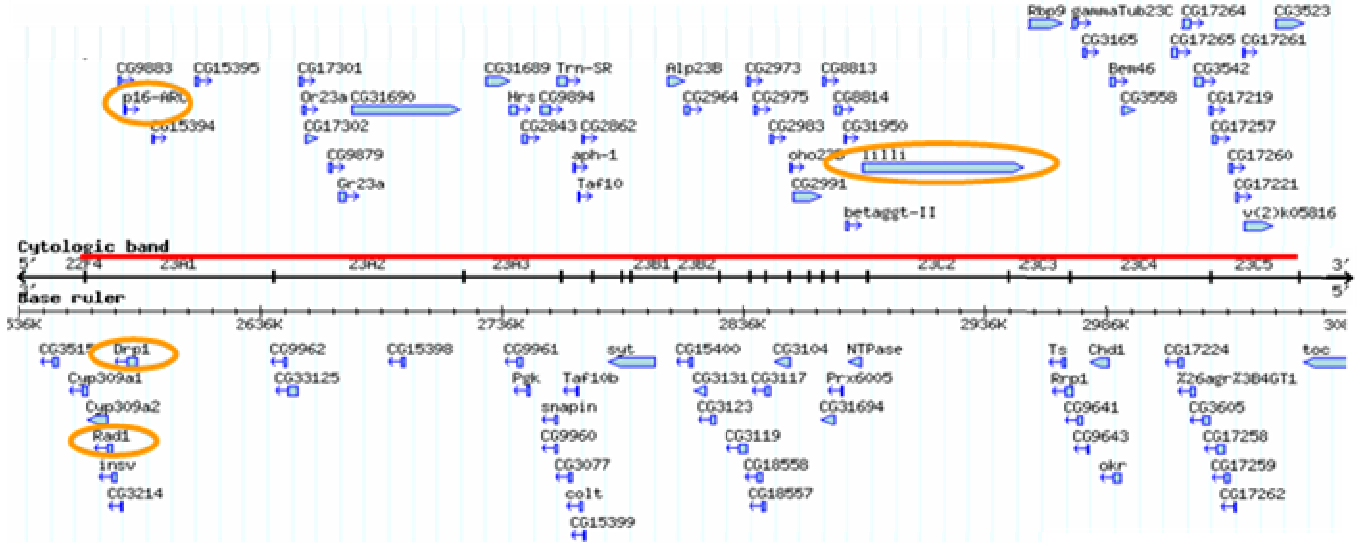
Cytologic band
Base ruler
CG9883
CG15395
CG17301
CG31689
Trn-SR
Alp23B
CG2973
CG8813
p16-ARC
CG15394
Or23a
CG31690
Hrs
CG9694
CG2964
CG2975
CG8814
CG17302
CG2843
CG2862
CG2983
CG31950
CG9879
aph-1
Gr23a
Taf10
CG2991
betaggt-II
11111
Rbp9
gammaTub23C
CG17264
CG3523
CG3165
CG17265
CG17261
Bem46
CG3542
CG3558
CG17219
CG17257
CG17260
CG17221
v(2)k05816
Drp1
Cyp309a1
Cyp309a2
Rad1
insv
CG3214
CG9962
CG33125
CG15398
CG9961
svt
Pgk
Taf10b
snapin
CG9960
CG3077
colt
CG15399
CG15400
CG3104
NTPase
CG3131
CG3117
Prx6005
CG3123
CG31694
CG3119
CG18558
CG18557
Ts
Chd1
Rrp1
CG9641
CG9643
okr
CG17224
toc
Z26agrZ3B4GT1
CG3605
CG17258
CG17259
CG17262

**Figure 5. 11:** *Schematic of the region responsible for the S81 interaction*

**A:** Polytene divisions 23, and 24 of chromosome 2L are indicated and sub-divisions within are shown. The deletion responsible for the S81 interaction is positioned closest to the chromosome schematic. Deletions that suppress the GMR>DRAD21$^{DM}$ eye phenotype are indicated by thick black lines, those that enhance the phenotype are indicated by thick grey lines, those that do not interact are indicated by thin black lines. A deletion that enhances the GMR>DRAD21$^{DM}$ phenotype (E240) is also shown. Breakpoints and deficiency names are shown under each deletion, and BL stock numbers in brackets. Breakpoints are mapped cytologically and in many cases are estimates only. The narrowed region likely to contain the suppressor locus/loci is indicated by the green block and is shown in more detail in B.
**B:** Molecular map of the region putatively containing the suppressor locus (red line, green block in A). Numerous genes are contained within this small region, including the candidate loci *Drp1*, *rad1*, *p16-ARC* and *lilli* (circled in orange). Gene names are indicated. Also shown is a cytological map and molecular coordinates within chromosome 2L. There are additional candidates that map to this region but are not indicated here as their precise position remains unclear.

Position effect variegation (PEV) is the inactivation of a gene in some cells through its abnormal juxtaposition with heterochromatin, usually through chromosome rearrangements. Suppressors and enhancers of PEV act by influencing the chromatin state by either increasing or decreasing the degree of heterchromatinisation respectively. *Su(var)2-4* maps to 23A3-D4 and therefore may fall within the defined suppressor interval. *Su(var)2-4* is a strong, dominant suppressor of PEV, however the mechanism by which this occurs is still unknown (Hwang et al., 2001, Wustmann et al., 1989). Its role in regulating the chromatin state made *Su(var)2-4* a candidate suppressor within this region, however the *Su(var)2-4$^{01}$* allele failed to modulate the GMR>DRAD21$^{DM}$ phenotype.

LILLIPUTIAN is a protein involved in the regulation of cell size and cytokinesis and is encoded by *lilli* located at 23B7-23C2. *lilli* genetically interacts with the *Pten* tumour suppressor gene, further supporting its role in the correct execution of the cell cycle, however, the *lilli$^{k05431}$* insertion allele failed to significantly modify the GMR>DRAD21$^{DM}$ phenotype.

The final two candidate suppressor loci identified in the 23A1;23C1-2 interval were initially identified in a genetic screen for modifiers of meiotic chromosome segregation and are named *Sensitised chromosome inheritance modifier 12* (*Scim12*) and *Sensitised chromosome inheritance modifier13* (*Scim13*) respectively (Dobie et

al., 2001). The exact gene corresponding to both of these mutations is not known, although it is likely that *Scim13* corresponds to CG9892, thought to encode an ATPase that forms part of the ABC transport complex. Homozygous *Scim12* mutants display mitotic defects with abnormal neuroblast metaphases in addition to the dominant modification of meiotic chromosome inheritance (Dobie et al., 2001). The $Scim12^{2}$ insertion allele failed to modify the GMR>DRAD21$^{DM}$ phenotype. The $Scim13^{1}$ insertion allele was capable of suppressing the size defect of the GMR>DRAD21$^{DM}$ phenotype and of weakly suppress the organisation defect (Figure 5.12). However, $Scim13^{1}$ was not capable of suppressing the GMR>DRAD21$^{DM}$ phenotype to the same extent as the original Df(2L)C144 deletion. These results indicate that the S81 interaction is due, at least in part, to the deletion of the *Scim13* gene, although, the existence of other weak modifier loci cannot be ruled out.

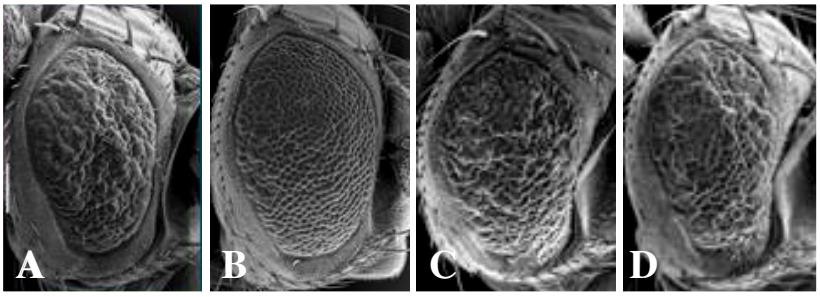


**Figure 5. 12:** *Mutations in Scim13 suppress the GMR>DRAD21$^{DM}$ eye phenotype*

Scanning electron micrographs of adult *Drosophila* eyes, dorsal side is up and anterior to the right. **A:** The reduced and roughened eye phenotype of GMR>DRAD21$^{DM}$. **B:** The organisation and size defects are suppressed by the introduction of Df(2L)C114 ( S81) **C** and **D:** Two examples of $Scim13^{1}$ mediated suppression of GMR>DRAD21$^{DM}$. The $Scim13^{1}$ insertion allele suppresses the size defect but does not significantly suppress the organisation defect.

#### 5.2.6.3 Proposed mechanism of suppression

*Scim13* was identified in a genetic screen for modifiers of meiotic chromosome segregation (Dobie et al., 2001). *Scim13* is thought to correspond to CG9892, an ATP-binding protein that forms part of the ABC transport complex; however its exact identity and function remain to be elucidated.

It remains unclear exactly how halving the dose of *Scim13* is able to dominantly suppress the GMR>DRAD21$^{DM}$ phenotype. However, identification of this locus as a dominant modifier of both meiotic and mitotic chromosome segregation (Dobie et al., 2001) indicates that SCIM13 is likely to play a direct role in chromosome segregation, presumably through regulation of the cohesin complex.

### 5.2.7 IDENTIFICATION OF *PROD* AS THE SUPPRESSOR LOCUS IN REGION S164

#### 5.2.7.1 S164 region overview

The S164 interaction belongs to the "Strong Suppressor" phenotypic category (Section 4.2.3.2). This phenotype is characterised by an increase in both the size and the organisation of the GMR>DRAD21$^{DM}$ eye phenotype resulting in an almost wild-type eye phenotype (Figure 4.8, Table 4.5).

The deficiency responsible for S164 (Df(2R)P34) was obtained from BL stock 757. This deficiency is on the right arm of the second chromosome and spans the polytene regions 55E2-4;56C1-11 deleting a minimum of 32 and maximum of 45 polytene bands and 61-92 genes. Analysis of the annotations of the genes mapped to this region indicate that there are six involved in the immune response and at least four genes encoding proteins involved in protein transport. A minimum of 23 genes within this region have an unknown function and are only known by their genome project (CG) number. Only 34 genes in this region have publicly available alleles.

#### 5.2.7.2 Genetic dissection of region S164

Two other Deficiency Kit deletions have breakpoints that overlap with that of Df(2R)P34. The first of these, Df(2R)PC4 has the breakpoints 55A1;55F1-2 and does not modify the GMR>DRAD21$^{DM}$ phenotype. This means that the suppressor locus for S164 cannot lie in the region that is common to these two deletions. The second deficiency, Df(2R)BSC26, has the breakpoints 55C4;55D6-10, and while this deletion suppresses the GMR>DRAD21$^{DM}$ eye phenotype the interaction is much weaker than that of the S164 suppression (Figure 5.13). The S91 interaction does not suppress the reduced size of the eye, whilst S164 suppresses both the size and organisation defects. This indicates that the locus responsible for the S164 interaction cannot lie within a region of the chromosome common to both deletions, or that the deficiency

responsible for the S91 interaction deletes additional loci that influence the GMR>DRAD21$^{DM}$ phenotype in an additive manner. Taken together these data refine the interval of interest down to 55F1-2;56C1-11 (Figure 5.14). This refined region deletes 23-34 polytene bands and 63 genes. There were four obvious candidate genes identified in this region including *prod, topors, CG15105* and *ena*.

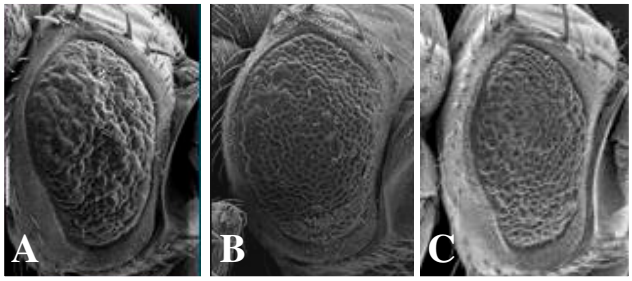


**Figure 5. 13:** *S164 and S91 suppress the GMR>DRAD21$^{DM}$ eye phenotype to different extents.*

Scanning electron micrographs of adult *Drosophila* eyes, dorsal side is up and anterior to the right. **A:** The reduced and roughened eye phenotype of GMR>DRAD21$^{DM}$. **B:** The GMR>DRAD21$^{DM}$ size and organisation defects are strongly suppressed by the introduction of Df(2R)P34 (S164). **C:** The introduction of Df(2R)BSC26 (S91) strongly suppresses the organisation but not the size defect of GMR>DRAD21$^{DM}$.

In assessing whether the reduced and roughened GMR>DRAD21$^{DM}$ was suitable for a genetic screen a range of second site mutations were introduced into this genetic background (Section 4.2.1). In the course of these experiments it was determined that the *prod$^{k08810}$* insertion allele was capable of weakly suppressing the reduced and roughened eye phenotype (Figure 5.15). These results indicate that the S164 suppression is due at least in part to the deletion of the *prod* locus.

Given that *prod* is only capable of weakly suppressing the GMR>DRAD21$^{DM}$ phenotype, it is likely that the strong suppression phenotype of S164 is due to a number of separate loci acting additively. Other loci likely to contribute to the S164 phenotype (in addition to *prod*) include *topors*, which encodes a Topoisomerase I interacting protein, *CG15105* which putatively encodes a ubiquitin ligase and *ena*, which is involved in regulating the cytoskeleton and cell shape.

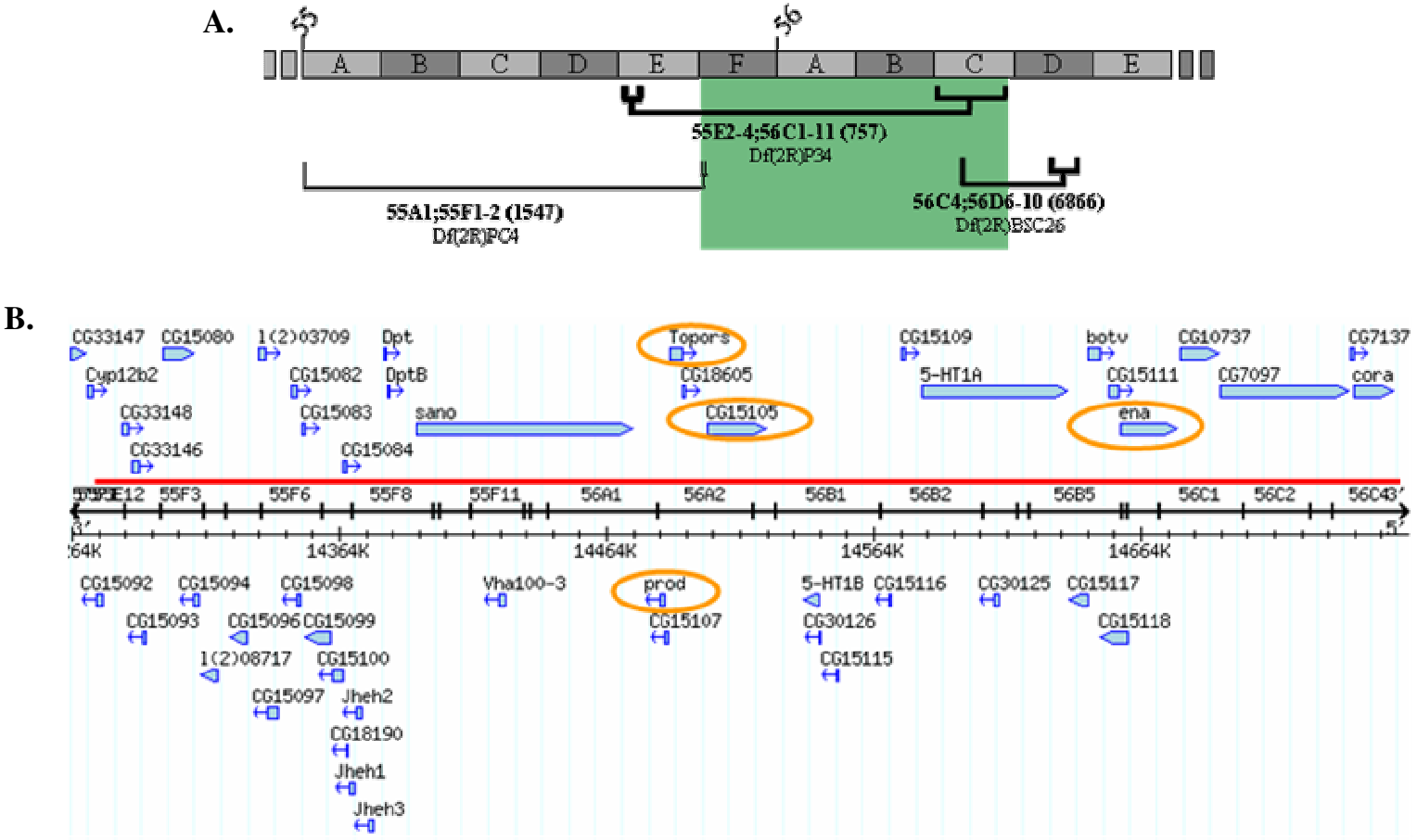
A.
55
56
A B C D E F A B C D E
55E2-4;56C1-11 (757)
Df(2R)P34
55A1;55F1-2 (1547)
Df(2R)PC4
56C4;56D6-10 (6866)
Df(2R)BSC26
B.
CG33147 CG15080 l(2)03709 Dpt Topors CG15109 botv CG10737 CG7137
Cyp12b2 CG15082 DptB CG18605 5-HT1A CG15111 CG7097 cora
CG33148 CG15083 sano CG15105 ena
CG33146 CG15084
55F3 55F6 55F8 55F11 56A1 56A2 56B1 56B2 56B5 56C1 56C2 56C43
14364K 14464K 14564K 14664K
CG15092 CG15094 CG15098 Vha100-3 prod 5-HT1B CG15116 CG30125 CG15117
CG15093 CG15096 CG15099 CG15107 CG30126 CG15118
l(2)08717 CG15100 CG15115
CG15097 Jheh2
CG18190
Jheh1
Jheh3

**Figure 5. 14:** *Schematic of the region responsible for the S164 interaction*

**A:** Polytene divisions 55, and 56 of chromosome 2R are indicated and sub-divisions within are shown. The deletion responsible for the S81 interaction is positioned closest to the chromosome schematic and all deletions shown form part of the Deficiency Kit. Deletions that suppress the GMR>DRAD21$^{DM}$ eye phenotype are indicated by thick black lines whilst non-modifiers are indicated as thin black lines. Breakpoints and deficiency names are shown under each deletion, and Bloomington stock numbers in brackets. Breakpoints are mapped cytologically and in many cases are estimates only. The narrowed region likely to contain the suppressor locus/loci is indicated by the green block and is shown in more detail in B. **B:** Molecular map of the region putatively containing the suppressor locus (red line corresponding to green block in A). Numerous genes are contained within this small region, including the candidate suppressors *prod, topors, CG15105* and *ena* (circled in orange). Prod insertion mutation *prod*$^{k08810}$, is capable of suppressing the GMR>DRAD21$^{DM}$ phenotype. Gene names are indicated. Also shown is a cytological map and molecular coordinates within chromosome 2L. There are additional candidates that map to this region but are not indicated here as their precise position remains unclear.

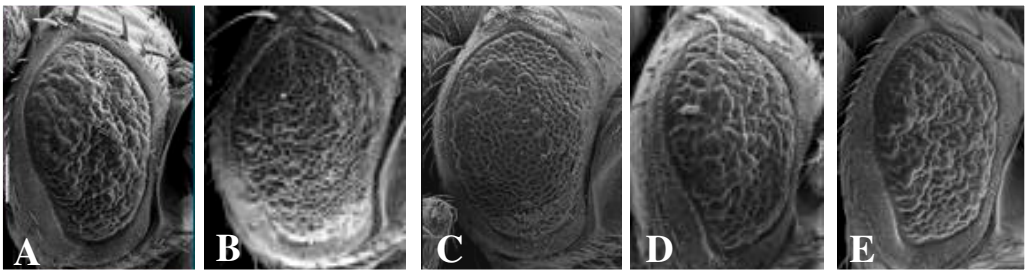


**Figure 5. 15:** *A prod insertion allele suppress the GMR>DRAD21$^{DM}$ eye phenotype*

Scanning electron micrographs of adult *Drosophila* eyes, dorsal side is up and anterior to the right. **A:** The reduced and roughened eye phenotype of GMR>DRAD21$^{DM}$. **B** and **C:** Two examples of Df(2R)P34 mediated GMR>DRAD21$^{DM}$ suppression. The size and organisation defects of GMR>DRAD21$^{DM}$ are strongly suppressed by the introduction of Df(2R)P34 (S81). **D** and **E:** Two examples of *prod*$^{k08810}$ mediated GMR>DRAD21$^{DM}$ suppression. The *prod*$^{k08810}$ insertion allele weakly suppresses the size and organisation defects of GMR>DRAD21$^{DM}$.

#### 5.2.7.3 Proposed mechanism of suppression

PROD is a DNA-binding protein indispensable for the formation of heterochromatin and cell proliferation, however, its precise role in these processes remains to be fully elucidated. During mitosis PROD is localised to centromeric heterochromatin, and during interphase associates with approximately 400 individual euchromatic loci (Torok et al., 2000, Torok et al., 1997). Therefore, the function of PROD may extend beyond chromosome condensation in the vicinity of the centromere to transcriptional regulation.

The mechanism by which halving the dose of *prod* is capable of suppressing the GMR>DRAD21$^{DM}$ is most likely related to its chromosome condensation role and may be similar to that discussed in section 5.2.4.3 for *HDAC4* mediated suppression. Halving the dose of *prod* could decrease the level of chromatin condensation in the vicinity of the centromere which in turn reduces the recruitment and/or efficacy of cohesin in the region. This weakening of centromeric cohesion can, in part, counteract the strengthening effect of DRAD21$^{DM}$ expression and therefore suppress the GMR>DRAD21$^{DM}$ eye phenotype. Further support for this hypothesis would be obtained by testing additional *prod* alleles and by analysing the distribution of cohesin proteins on chromosomes of *prod* mutants. The contribution of any additional loci to the S81 phenotype remains to be assessed.

### 5.2.8 IDENTIFICATION OF *CDK7* AS THE SUPPRESSOR LOCUS IN REGIONS S82 AND S158

#### 5.2.8.1 S82 and S152 regions and genetic dissection

The deficiencies responsible for S82 and S158 are Df(1)JC70 and Df(1)A113 respectively. These deletions overlap extensively and modify the GMR>DRAD21$^{DM}$ phenotype to similar extents, strongly suppressing the size and organisation defects (Figure 5.16; and discussed in Chapter 4, section 4.2.2.2). It is therefore likely that the interactions observed are due to a single locus or region, defining the interacting interval as most probably being the region common to both deletions. This theory was confirmed by testing two additional deletions, one of which, Df(1)BA2-8, also forms part of the Deficiency Kit and does not modify the GMR>DRAD21$^{DM}$

phenotype. The Df(1)dm75e19 Deficiency Kit deletion has breakpoints that overlap with those of Df(1)A113 and suppresses the GMR>DRAD21$^{DM}$ phenotype. This suppressing region, named S72, and is not as strong as either S82 or S158 and is likely to be caused by the deletion of a separate locus (Figure 5.16). These data define the interacting region as spanning 4C15-16;4F5 (Figure 5.17). This refined region consists of a minimum of 32 polytene bands encoding a minimum of 45 genes, approximately half of which are known by CG number only, and only 12 genes in this region have publicly available alleles. Analysis of the annotations of the 45 genes in the narrowed interval allowed five candidate genes to be identified (Figure 5.17), including *Bteb2, rg, Mcm3, XRCC1* and *Cdk7*.

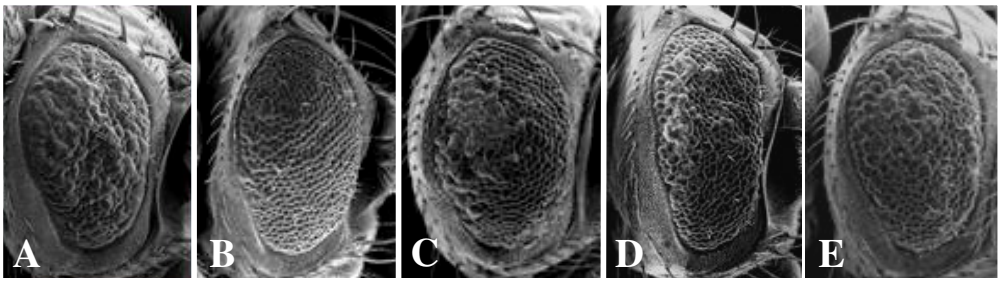


**Figure 5. 16:** *S82 and S158 suppress the GMR>DRAD21$^{DM}$ eye phenotype to similar extents*

Scanning electron micrographs of adult *Drosophila* eyes, dorsal side is up and anterior to the right. **A:** The reduced and roughened eye phenotype of GMR>DRAD21$^{DM}$. **B** and **C:** The size and organisation defects of GMR>DRAD21$^{DM}$ are strongly suppressed by the introduction of Df(1)JC70 (S82) and Df(1)A113 (S158) respectively. **D** and **E:** The size and organisation defects of GMR>DRAD21$^{DM}$ are moderately suppressed by the introduction of the Deficiency kit deletion Df(1)dm75e19 (S72) the additional deletion Df(1)ovo44, respectively.

**A.**

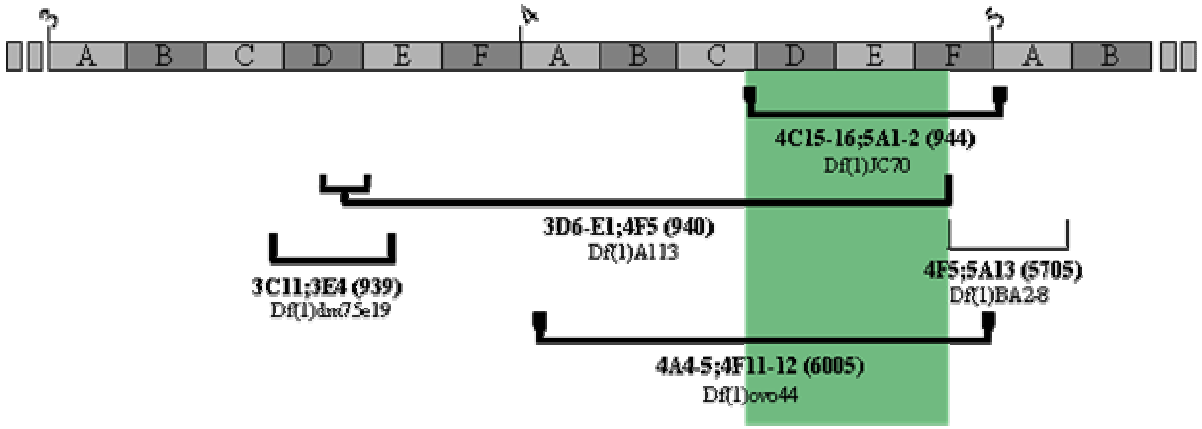
A B C D E F A B C D E F A B
4C15-16;5A1-2 (944)
Df(1)JC70
3D6-E1;4F5 (940)
Df(1)A113
3C11;3E4 (939)
Df(1)dx75e19
4F5;5A13 (5705)
Df(1)BA2-8
4A4-5;4F11-12 (6005)
Df(1)ovo44

**B.**

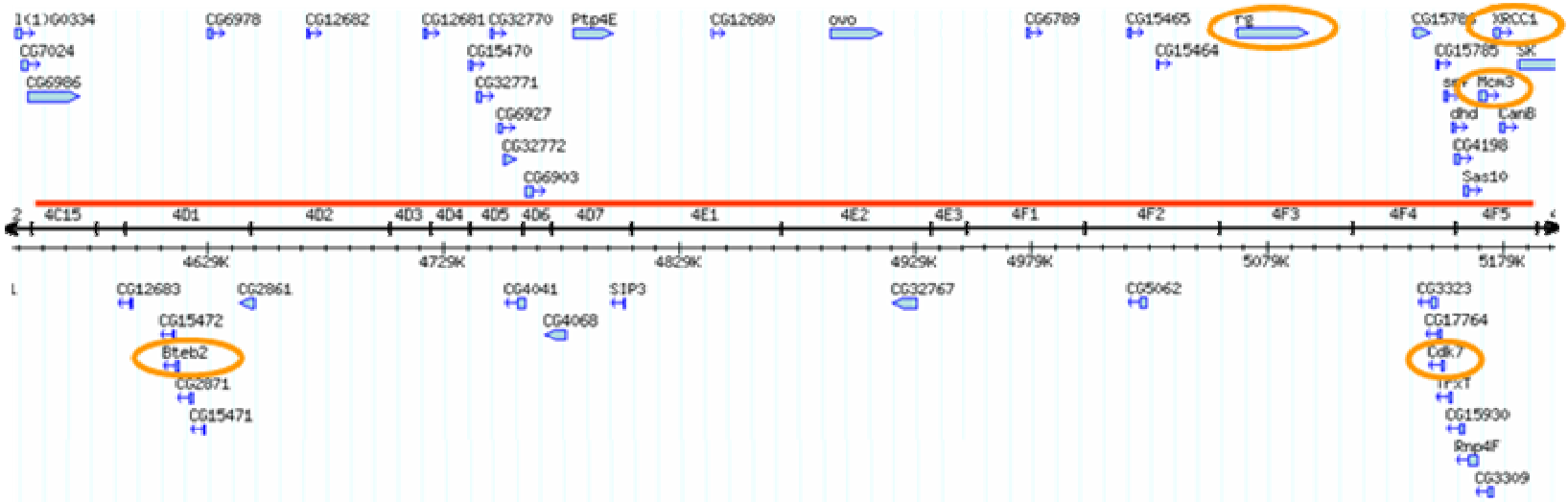
CG7024
CG6986
CG6978
CG12682
CG12681
CG32770
CG15470
CG32771
CG6927
CG32772
CG6903
Ptp4E
CG12680
ovo
CG6789
CG15465
CG15464
XRCC1
Rcm3
CG4198
Sas10
4C15
4D1
4D2
4D3
4D4
4D5
4D6
4D7
4E1
4E2
4E3
4F1
4F2
4F3
4F4
4F5
4629K
4729K
4829K
4929K
4979K
5079K
5179K
CG12683
CG2861
CG15472
Bteb2
CG2871
CG15471
CG4041
SIP3
CG4068
CG32767
CG5062
CG3323
CG17764
Cdk7
CG15930
Rnp4F
CG3309

**Figure 5. 17:** *Schematic of the region responsible for the S82 and S158 interactions*

**A:** Polytene divisions 3, 4 and 5 of chromosome 1 (X) are indicated and sub-divisions within are shown. The deletion responsible for the S82 interaction is positioned closest to the chromosome schematic, and the deletion responsible for the S158 interaction is shown directly under it. Deletions that suppress the GMR>DRAD21$^{DM}$ eye phenotype are indicated by thick black lines, whist those that do not modify the phenotype are indicated by thin black lines. Breakpoints and deficiency names are shown under each deletion, as are the Bloomington stock numbers. Breakpoints are mapped cytologically and in many cases are estimates only. The deletions obtained from stocks 939 and 5705 are part of the Deficiency Kit and the former is responsible for the S72 interaction. The additional deletion shown (Df(1)ovo44) was obtained and tested to aid in the interpretation of the Deficiency Kit screen results. The narrowed region likely to contain the suppressor locus/loci is indicated by the green block and is shown in more detail in B.
**B:** Molecular map of the region putatively containing the suppressor locus (red line corresponds to the green block in A). Numerous genes are contained within this small region, including the candidate suppressors *Bteb2, rg, Mcm3, XRCC1* and *Cdk7* (circled in orange). Gene names are indicated. Also shown is a cytological map and molecular coordinates within chromosome 2L.

---

The contribution of the *Bteb2, Mcm3* and *XRCC1* candidate loci to the S82 and S158 suppression phenotypes was unable to be tested due to the lack of publicly available alleles. Alleles that were obtained and tested directly included $rg^{KG02343}$ and a null allele of *Cdk7*.

*rg* (*rugose*) located at 4F3 encodes a protein kinase A binding protein that is involved in the specification of cone and photoreceptor cells in the eye. *Rg* is expressed in nearly all tissues throughout the development of the fly, interacts with both the Notch and EGFR signalling pathways and is involved in controlling development (Shamloula et al., 2002, Han et al., 1997). The insertion allele $rg^{KG02343}$ was obtained and shown to be incapable of suppressing the GMR>DRAD21$^{DM}$ phenotype.

*Cdk7*, located at 4F4, encodes a cyclin dependent kinase that is essential for mitosis and required for the activation of the key mitotic cyclin complexes, CDC2/CYCLINA and CDC2/CYCLINB (Larochelle et al., 1998, Alphey et al., 1992, Perdiguero and Nebreda, 2004). Its role in regulating mitotic entry makes *Cdk7* a prime candidate suppressor in this region, and the *Cdk7* null allele obtained from BL stock 4557 was capable of suppressing the size defect but not the organisation of the GMR>DRAD21$^{DM}$ phenotype (Figure 5.18). These results indicate that the S82/S158 interaction is due at least in part to the deletion of the *Cdk7* gene.


**Figure 5. 18:** *A Cdk7 null allele suppresses the GMR>DRAD21$^{DM}$ eye phenotype*

Scanning electron micrographs of adult *Drosophila* eyes, dorsal side is up and anterior to the right. **A:** The reduced and roughened eye phenotype of GMR>DRAD21$^{DM}$. **B** and **C:** The size and organisation defects of GMR>DRAD21$^{DM}$ are strongly suppressed by the introduction of Df(1)JC70 (S82) and Df(1)A113 (S158) respectively**. D:** The introduction of a *Cdk7* null allele strongly suppresses the size but not the organisation defect of GMR>DRAD21$^{DM}$.

#### 5.2.8.1 Proposed mechanism of suppression

CDK7 performs two different but essential functions in *Drosophila*. Firstly, CDK7 is part of the TFIIH transcription factor complex (Leclerc et al., 2000, Aoyagi and Wassarman, 2000) and CDK7 activity in this complex is required for the transcription of some promoters *in vivo* (Akoulitchev et al., 1995). Secondly, CDK7 is a Cdk-activating-kinase, with specific activity directed toward the CDC2 kinase partner of mitotic cyclins (Larochelle et al., 1998). Given that halving the dose of both *cycA* and *cycB* suppress the GMR>DRAD21$^{DM}$ phenotype it is likely that the ability of *cdk7* to suppress the GMR>DRAD21$^{DM}$ phenotype is related to its function in regulating CDC2 activity.

In CDK7 mutant embryos CYCLIN A/CDC2 complexes are unstable and the activity of CYCLIN B/CDC2 complexes are reduced (Larochelle et al., 1998). Therefore, halving the dose of *Cdk7* may be suppressing the GMR>DRAD21$^{DM}$ phenotype indirectly through a reduction in the activity of the mitotic CYCLIN/CDC2 complexes. Alternatively, a half dose of *Cdk7* may be sufficient to maintain optimal levels of mitotic CYCLIN/CDC2 activity. If this is the case the observed suppression may be mediated by the requirement of CDC7 activity for the expression of a cell cycle regulator, or cohesin regulator, critical for correct chromosome segregation. Arguing against this alternative hypothesis is the observation that CDK7 activity is

not required for the transcription of mitotic or S-phase cyclins (Larochelle et al., 1998), however other potential CDK7 transcriptional targets have not been studied. Taken together the results of halving the dose of *cycA, cycB* and *Cdk7* provide strong, if circumstantial, evidence that the *Cdk7* suppression of the GMR>DRAD21$^{DM}$ phenotype is due to decreased activity of CDC2.

### 5.2.9 IDENTIFICATION OF *kni* AS THE ENHANCER LOCUS IN REGION E97

#### 5.2.9.1 E97 region overview

The E97 interaction belongs to the "Strong Enhancer" phenotypic category (section 4.2.3.3) and is characterised by a dramatic decrease in both the size and organisation of the GMR>DRAD21$^{DM}$ eye phenotype (Figure 4.10, Table 4.6).

The deficiency responsible for E97 (Df(3L)ri-XT1) was obtained from BL stock 5878. This deficiency is on the left arm of the third chromosome and spans the polytene regions 77E2-4;78A2-4 deleting a minimum of 12 and maximum of 16 polytene bands, and at least 41-44 genes. Analysis of the annotations of the genes mapped to this region indicate that a minimum of 25 genes have an unknown function and are only known by their genome project (CG) number and only 18 have publicly available alleles.

#### 5.2.9.2 Genetic dissection of region E97

Two other Deficiency Kit deletions have breakpoints that overlap with that of Df(3L)ri-XT1. The first of these, Df(3L)ME107, has the breakpoints 77F3;78C8-9 and does not modify the GMR>DRAD21$^{DM}$ phenotype. This means that the enhancer locus in region E97 cannot lie in the region that is common to these two deletions. The second deficiency, Df(3L)ri-79c, has the breakpoints 77B-C;77F-78A, and this deletion enhances the GMR>DRAD21$^{DM}$ eye phenotype (E99 was not investigated further). The E99 interaction does not enhance the reduced size of the eye, whilst E97 enhances both the size and organisation defects (Figure 5.19). In addition, the E97 eye has a smoother surface than that of the E99, indicating that there are fewer differentiated ommatidia in the eye when GMR>DRAD21$^{DM}$ is expressed in the presence of the Df(3L)ri-XT1 deletion. This indicates that the locus responsible for the E97 interaction cannot lie within a region of the chromosome common to both

deletions, or that additional loci in the E99 deletion are also influencing the phenotype. The breakpoints of the deletion responsible for the E99 interaction are only vaguely defined and are of no assistance in narrowing down the interacting interval for E97.

Using the data from the first deficiency, Df(3L)ME107, the interacting region is refined to 77E2-4;77F3 (Figure 5.20). This narrowed region deletes a minimum of 8 polytene bands. Three candidate genes were identified in this region including *Pitslre, CSN3* and *kni* (Figure 5.20).

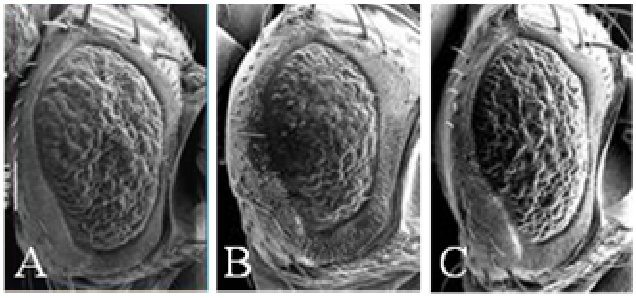


**Figure 5. 19:** *E97 and E99 enhance the GMR>DRAD21$^{DM}$ eye phenotype to different extents*

Scanning electron micrographs of adult *Drosophila* eyes, dorsal side is up and anterior to the right. **A:** The reduced and roughened eye phenotype of GMR>DRAD21$^{DM}$. **B:** The GMR>DRAD21$^{DM}$ eye is further reduced and lacks ommatidial structures by the introduction of (Df(3L)ri-XTI (E97). **C:** The Df(3L)ri-79c (E99) also enhances the organisation defects of the GMR>DRAD21$^{DM}$ phenotype but has little effect on the size of the eye.

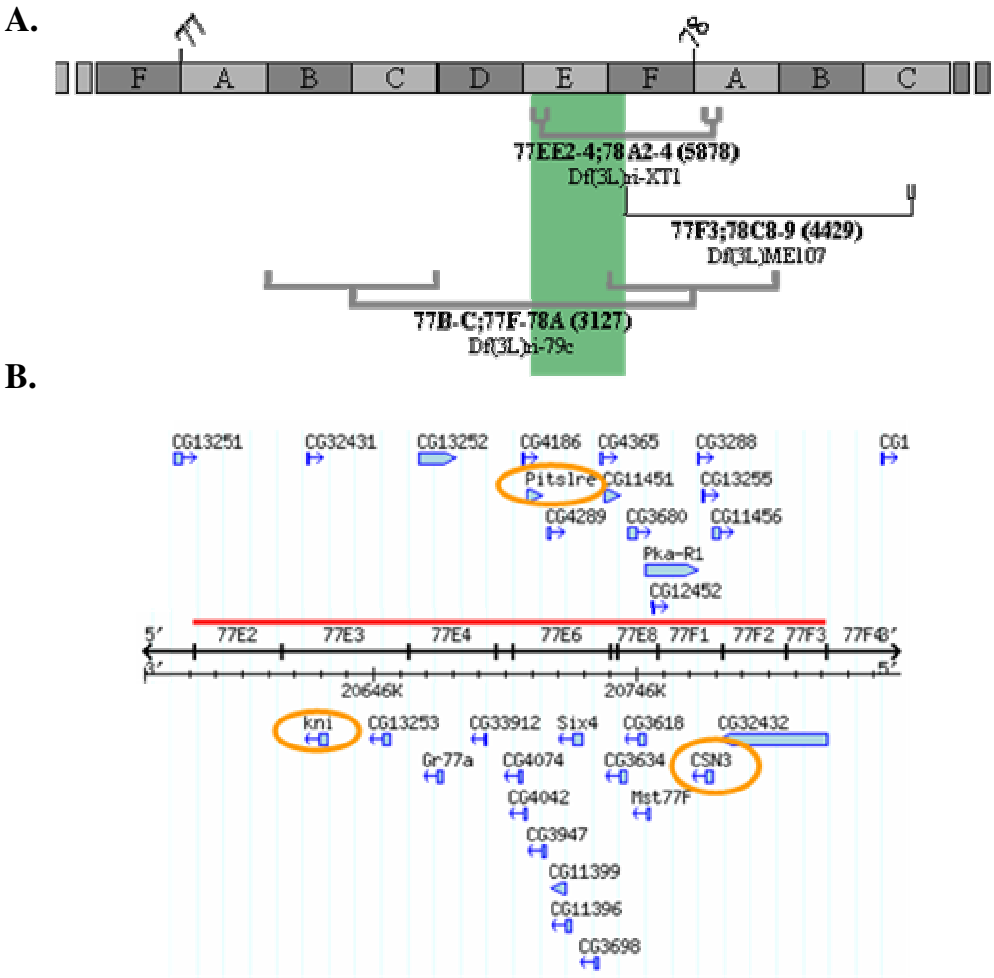


**Figure 5. 20:** *Schematic of region deleted to produce the E97interaction*

**A:** Polytene divisions 77 and 78 of chromosome 3L are indicated and sub-divisions within are shown. The deletion responsible for the E97 interaction is positioned closest to the chromosome schematic, and the deletion responsible for the E99 interaction is shown at the bottom. Deletions that enhance the GMR>DRAD21$^{DM}$ eye phenotype are indicated by thick grey lines and those that do not interact are indicated by thin black lines. Breakpoints and deficiency names are shown under each deletion, as are the Bloomington stock numbers (brackets). Breakpoints are mapped cytologically and in many cases are estimates only. All deletions shown comprise part of the Deficiency Kit. The narrowed region likely to contain the suppressor locus/loci is indicated by the green block and is shown in more detail in B.
**B:** Molecular map of the region putatively containing the suppressor locus (red line corresponds to the green block in A). Numerous genes are contained within this small region, including the candidate suppressors *Pitslre, CSN3* and *kni* (circled in orange). Gene names are indicated. Also shown is a cytological map and molecular coordinates within chromosome 2L.

The contribution of *Pitslre*, a Cdc2-related kinase putatively involved in the regulation of the cell cycle and mitosis, to the E97 phenotype was unable to be assessed due to the lack of publicly available alleles. This was also the case for the Cop9 encoding *CSN3*, which is involved in proteasome regulation.

A third, and final, candidate gene identified in this region was *kni*, located at 77E3. *kni* encodes the KNIRPS transcriptional repressor implicated in mitotic regulation (Fuss et al., 2001). Both the weak *kni* allele, $kni^{ri\text{-}1}$, and the null allele $kni^{10}$ enhanced the GMR>DRAD21$^{DM}$ eye phenotype, although neither to the same extent as the original deficiency, Df(3L)ri-XT1 (Figure 5.21). These data indicate that the E97 phenotype is at least in part due to the deletion of *kni*.

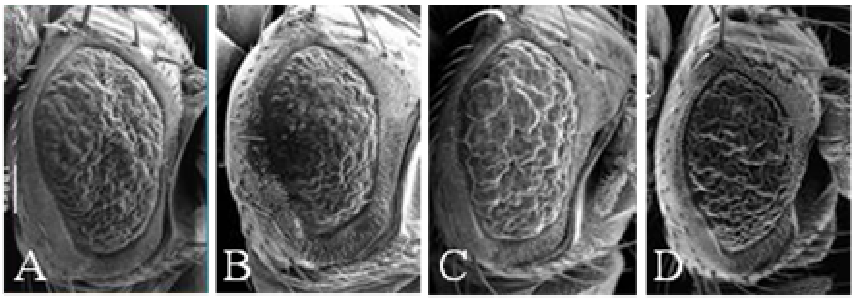


**Figure 5. 21:** *Two different kni alleles enhance the GMR>DRAD21$^{DM}$ eye phenotype*

Scanning electron micrographs of adult *Drosophila* eyes, dorsal side is up and anterior to the right. **A:** The reduced and roughened eye phenotype of GMR>DRAD21$^{DM}$. **B:** The GMR>DRAD21$^{DM}$ phenotype is strongly enhanced by the introduction of Df(3L)ri-XT1 (E79). **C** and **D:** The size and organisation defects of the GMR>DRAD21$^{DM}$ phenotype are also enhanced by the *kni* alleles, $kni^{10}$ and $kni^{ri\text{-}1}$ respectively.

#### 5.2.9.3 Proposed mechanism of enhancement

The function of KNIRPS has been studied most extensively in *Drosophila* embryogenesis where it is necessary for correct segmentation (Nauber et al., 1988, Strecker et al., 1991). In the *Drosophila* larval fore- and hind-gut, KNIRPS functions to transcriptionally repress S-phase genes and to prevent mitotic cells entering into endoreplication cycles (Fuss et al., 2001). Levels of the CYCLIN E induced S-phase proteins, such as PCNA and DNA-polymerase α are elevated in *kni* mutant cells (Fuss et al., 2001). Therefore the function of KNI in the developing gut is to oppose the effects of CYCLIN E expression in cells that are still mitotically cycling. It is anticipated that halving the dose of *kni* would result in an increase in S-phase proteins such as PCNA. If this is the case the enhancement of the GMR>DRAD21$^{DM}$ phenotype observed can be explained by a increase in the number of mitoses occurring in the affected cells, similar to that observed upon overexpression of CYCLIN E (Chapter 3, Figure 3.11). This hypothesis could be tested directly by quantifying the number of mitoses occurring in both wild-type and *kni* mutant eye discs using a stain for mitotic cells such as phospho-histone 3. These data provide the first evidence of the conservation of the *kni* S–phase repressive role in the eye imaginal disc, and raise the possibility that this a general mechanism used by mitotic cells to prevent premature S-phase entry.

### 5.2.10 COMPLEX GENETIC INTERACTIONS IN ENHANCER REGION E60

#### 5.2.10.1 E60 region overview

The E60 interaction belongs to the "Strong Enhancer" phenotypic category (Section 4.2.3.3) and is characterised by a dramatic decrease in both the size and organisation of the GMR>DRAD21$^{DM}$ eye phenotype (Figure 4.10, Table 4.6).

The deficiency responsible for E60 (Df(2R)nap9) was obtained from BL stock 1007. This deficiency is on the right arm of the second chromosome and spans the polytene regions 42A1-2;42E6-F1 deleting a minimum of 44 and maximum of 48 polytene bands, and at least 138-152 genes. Analysis of the genes mapped to this region indicate that a minimum of 36 genes have an unknown function and are only known by their genome project (CG) number and 23 encode tRNAs. Only 56 genes in this region have publicly available mutant alleles.

#### 5.2.10.2 Genetic dissection of region E60

Two other Deficiency Kit deletions have breakpoints that overlap with that of Df(2R)nap9, neither of which modify the GMR>DRAD21$^{DM}$ eye phenotype. The first of these, In(2R)bw$^{VDe2l}$Cy$^{R}$ has the breakpoints 41A-B;42A2-3, and the second deficiency, Df(2R)ST1, has the breakpoints 42B3-5;43E15-18. This means that the enhancer locus for E60 must lie within the region deleted exclusively in the Df(2R)nap9 deficiency.

Using the data from these overlapping Deficiency Kit deletions, the interacting region was narrowed down to 42A2;42B3-5 (Figure 5.22). This region deletes 21-23 polytene bands and a minimum of 53 genes. Seven obvious candidate genes were identified in this region, including *CG3043, dream, Bub1, Act42A, Src42A, Mle* and *EcR*.

**A.**

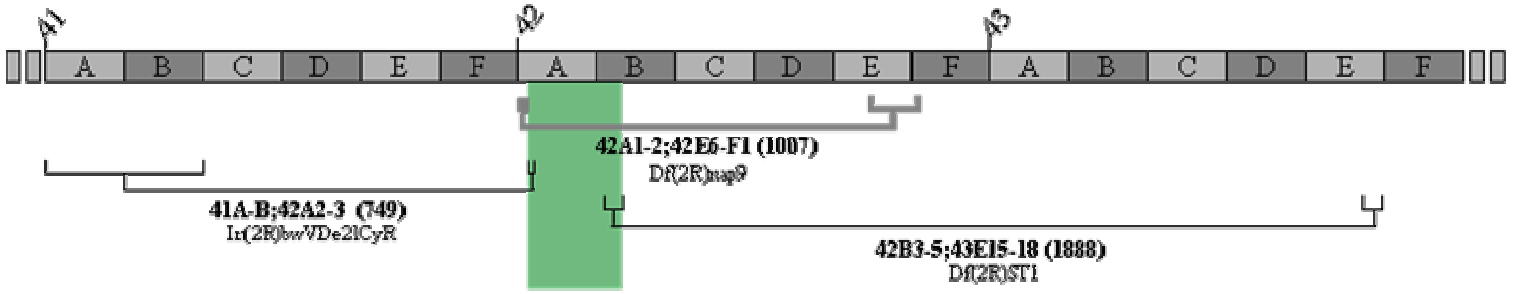
41
42
43
A B C D E F A B C D E F A B C D E F
42A1-2;42E6-F1 (1007)
Df(2R)exp9
41A-B;42A2-3 (749)
In(2R)bwVDe2lCyR
42B3-5;43E15-18 (1888)
Df(2R)ST1

**B.**

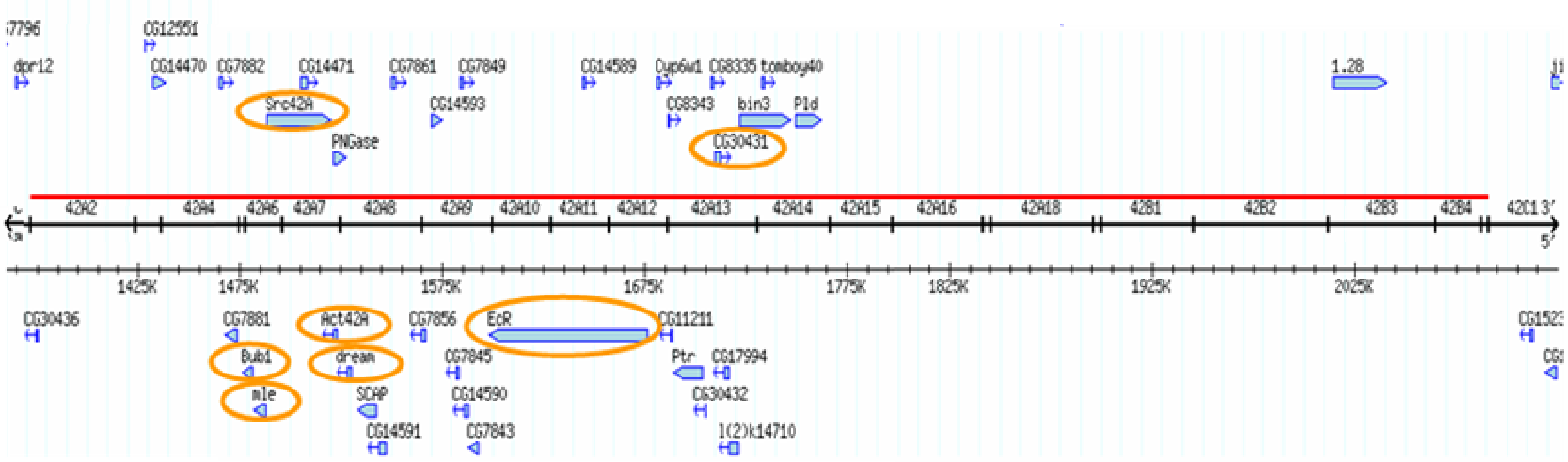
dpr12
CG14470
CG7882
CG14471
CG7861
CG7849
CG14589
Cyp6w1
CG8335
tomboy40
1.28
Src42A
CG14593
CG8343
bin3
Pld
PNGase
CG30431
42A2
42A4
42A6
42A7
42A8
42A9
42A10
42A11
42A12
42A13
42A14
42A15
42A16
42A18
42B1
42B2
42B3
42B4
1425K
1475K
1575K
1675K
1775K
1825K
1925K
2025K
CG30436
CG7881
Act42A
CG7856
EcR
CG11211
Bub1
dream
CG7845
Ptr
CG17994
mle
SCAP
CG14590
CG30432
CG14591
CG7843
l(2)k14710

**Figure 5. 22:** *Schematic of region deleted to produce the E60 interaction*

**A:** Polytene divisions 41, 42 and 43 of chromosome 2R are indicated and sub-divisions within are shown. The deletion responsible for the E60 interaction is positioned closest to the chromosome schematic. Deletions that enhance the GMR>DRAD21$^{DM}$ eye phenotype are indicated by thick grey lines, whilst those that do not interact are indicated as thin black lines. Breakpoints and deficiency names are shown under each deletion, as are the Bloomington stock numbers (brackets). Breakpoints are mapped cytologically and in many cases are estimates only. All deletions shown comprise part of the Deficiency Kit. The narrowed region likely to contain the suppressor locus/loci is indicated by the green block and is shown in more detail in B.
**B:** Molecular map of the region putatively containing the suppressor locus (red line corresponds to green block in A). Numerous genes are contained within this small region, including the candidate suppressors *CG3043, dream, Bub1, Act42A, Src42A, Mle* and *EcR* (circled in orange). Gene names are indicated. Also shown is a cytological map and molecular coordinates within chromosome 2L.

The contribution of candidate genes *CG30431*, putatively involved in cell proliferation, and the caspase, *dream,* to the E60 phenotype was unable to be assessed due to the lack of publicly available mutant alleles. Given that E60 was not eliminated from further analysis in the second-pass screen for modifiers of apoptosis (Chapter 4), it is unlikely that the deletion of *dream* is responsible for the E60 phenotype.

*Bub1*, located at cytological position 42A1-2 , encodes a serine threonine kinase that is part of the spindle checkpoint and therefore directly involved in chromosome segregation and mitotic exit (Basu et al., 1999). *Bub1* has been shown to genetically interact with *polo* (Garner et al., 2001) and *dup* (Donaldson et al., 2001), both of which have been shown to suppress the GMR>DRAD21$^{DM}$ eye phenotype (this study), further supporting the identification of *Bub1* as a candidate enhancer locus. The *Bub1*$^{k03113}$ hypomorphic insertion allele, however, was not capable of modulating the GMR>DRAD21$^{DM}$ eye phenotype.

*Act42A*, located at 42A4, encodes an actin protein involved in the biogenesis and organisation of the cytoskeleton. The *Act42A*$^{EY05608}$ insertion allele failed to modify the GMR>DRAD21$^{DM}$ phenotype.

*Mle*, located at 42A2, is an ATP-dependent DNA and RNA helicase involved in dosage compensation (Bone et al., 1994, Lasko, 2000, Schutt and Nothiger, 2000). Genetic interactions with *Shi*, which is known to be involved in microtubule binding

and through RNAi experiments has recently been shown to be required for cytokinesis, implicates *Mle* in these processes also. The $mle^{9}$ and $mle^{1}$ loss-of-function alleles modulated the GMR>$DRAD21^{DM}$ eye phenotype to a similar, if not further, extent as the Df(2R)nap9 deficiency responsible for the E60 interaction (Figure 5.23). These results indicate that the deletion of *mle* is at least in part responsible for the E60 interaction.

*EcR*, located at 42A9-13, transcription factor that as part of the ecdysone receptor holocomplex is involved in developmental events associated with moulting and metamorphosis, including imaginal disc eversion (Gibson and Schubiger, 2001, Carney and Bender, 2000, D'Avino and Thummel, 2000, Li and Bender, 2000). The $EcR^{V559fs}$ allele, which has a frameshift mutation in the ligand binding domain, and the $EcR^{225}$ null allele, enhance the GMR>$DRAD21^{DM}$ eye phenotype (Figure 5.23). These results indicate that the E60 phenotype is in part due to the reduced ability of the cells to respond to the ecdysone ectosteroid.

The *Src42A* oncogene, located at 42A6-7 encodes a protein-tyrosine kinase involved in eye morphogenesis and cell cycle regulation (Takahashi et al., 1996). Overexpression or inappropriate activation of *Src42A* induces ectopic proliferation (Pedraza et al., 2004, Read et al., 2004), and overexpression of *Src42A* also triggers apoptosis in a dose dependent manner. The $Src42A^{KG02515}$ insertion allele, $Src42A^{myri}$ myristylation mutant and the $Scr42A^{E1}$ truncation mutant are all capable of suppressing the GMR>$DRAD21^{DM}$ eye phenotype (Figure 5.23 and data not shown). $Src42A^{KG02515}$ suppresses both the size and organisation defects, whilst $Scr42A^{myri}$ and $Src42A^{E1}$ suppress the size defect only.

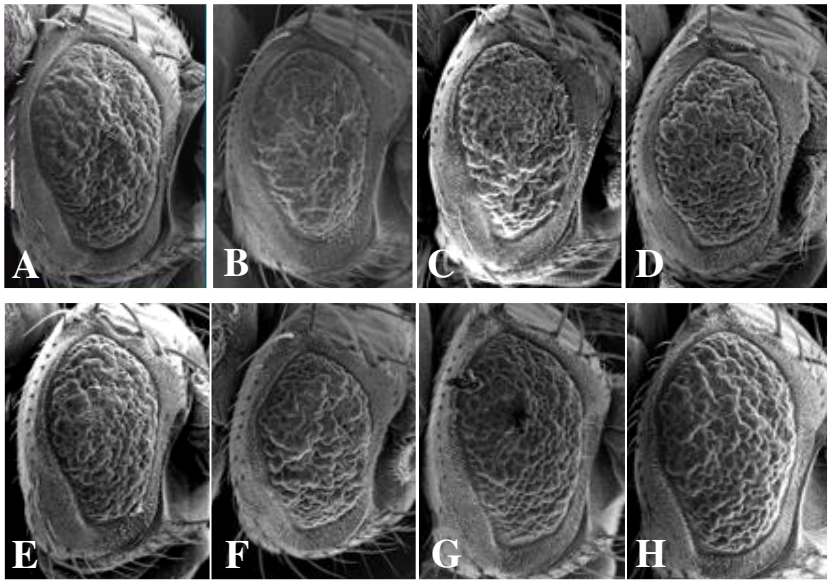


**Figure 5. 23:** *Different genetic interactions act together in region E60 to produce the observed enhancement phenotype*

Scanning electron micrographs of adult *Drosophila* eyes, dorsal side is up and anterior to the right. **A:** The reduced and roughened eye phenotype of GMR>DRAD21$^{DM}$. **B:** The GMR>DRAD21$^{DM}$ phenotype is strongly enhanced by the introduction of Df(2R)nap9 (E60). **C** and **D:** The size and organisation defects of the GMR>DRAD21$^{DM}$ phenotype are also enhanced by the *mle* alleles, *mle*$^{9}$ and *mle*$^{1}$ respectively. **E** and **F:** The size and organisation defects of the GMR>DRAD21$^{DM}$ phenotype are also enhanced by the *EcR* alleles *EcR*$^{V559fs}$ and *EcR*$^{225}$ respectively. **G** and **H:** The size and organisation defects of the GMR>DRAD21$^{DM}$ phenotype are mildly suppressed by the *Src42A* alleles *Src42A*$^{E1}$ and *Src42A*$^{myri}$.

### 5.2.10.3 Proposed mechanisms of interaction

The results presented for region E60 highlight that the data obtained from screening the Deficiency Kit are a sum of the effects of halving the dose, of all of the genes within the region of the deficiency. These data clearly show that it is possible for opposing interactions with more than one locus to arise within a genetically defined interval.

*5.2.10.3.1 Proposed mechanism of enhancement by mle*

It is unclear exactly how halving the dose of *mle* enhances the GMR>DRAD21$^{DM}$ phenotype. MLE is a DEAD box RNA helicase with reported roles in regulating the expression of both autosomal and X-linked genes by regulating the spatial distribution of acetylases. It was originally proposed that MLE was specifically involved in male dosage compensation due to its male-specific lethal mutant phenotype. Subsequent examination of gene expression in *mle* mutants shows that dosage compensation still occurs; however, there is a general trend of an increase in autosomal gene expression. Analysis of MLE protein distribution showed that it is not only present in female flies, but uniformly distributed along the chromosomes, whilst in males it is sequestered to the X chromosome (Hiebert and Birchler, 1994). Therefore the roles of MLE in dosage compensation, chromatin modification and gene expression remain unclear.

In addition to these roles, a gain of function *mle* allele, *mle$^{napts}$*, exhibits neurological defects due to altered sodium channel activity. At elevated temperatures *mle$^{napts}$* flies become paralysed, due to aberrant RNA editing of the *paralytic* transcript (Reenan et al., 2000). Therefore, the RNA helicase activity of *mle* is presumably required for the correct expression of at least some genes, such as *paralytic*.

Halving the dose of *mle* may enhance the GMR>DRAD21$^{DM}$ either through chromatin remodeling and/or through its function as an RNA helicase. Alternatively, this interaction may unveil yet another role for MLE in regulation of chromosome segregation.

*5.2.10.3.2 Proposed mechanism of enhancement by EcR*

EcR is involved in developmental events associated with pulses of ecdysone including moulting, metamorphosis and imaginal disc eversion (Gibson and Schubiger, 2001, Carney and Bender, 2000, D'Avino and Thummel, 2000, Li and Bender, 2000). EcR forms a heterodimeric ecdysone receptor complex with the *Drosophila* Retinoid X Receptor ULTRASPIRACLE (USP). DNA binding by the

ecdysone receptor complex is highly dynamic and co-operative, with EcR and USP combining with the SIN3/RPD3 histone deacetylase complex to influence gene expression (Arbeitman and Hogness, 2000, Tsai et al., 1999). *Drosophila* USP has been shown to be required to regulate the progression of the morphogenetic furrow, and in USP mutants furrow progression and differentiation occur more quickly. The role of USP in furrow progression may be direct, and involve EcR as a binding partner, as this complex has been demonstrated to repress basal level transcription (Zelhof et al., 1997). Halving the dose of *EcR* could therefore be acting similarly to USP mutants and increasing the rate of MF progression and differentiation. The enhancement of the GMR>DRAD21$^{DM}$ phenotype observed upon halving the dose of *EcR* could be due to a subsequent reduction in the amount of time that cells spend in mitosis and therefore a reduction in the amount of time available in anaphase to resolve the cohesion between sister chromatids. This is supported by the fact that mutations in *CycB* or *CycA*, that presumably slow the rate of mitotic progression, act to suppress the GMR>DRAD21$^{DM}$ eye phenotype.

*5.2.10.3.3 Proposed mechanism of suppression by Src42A*

*Src42A* is a proto-oncogene, that encodes a non-receptor protein-tyrosine kinase involved in eye morphogenesis and cell cycle regulation (Takahashi et al., 1996). Overexpression or inappropriate activation of *Src42A* induces ectopic proliferation (Pedraza et al., 2004, Read et al., 2004), and overexpression of *Src42A* also triggers apoptosis in a dose dependent manner. In *Drosophila* SRC42A has been implicated in negatively regulating the responses of the MAPK cascade (Lu and Li, 1999), however, this is inconsistent with its observed role as a positive regulator of cell proliferation and therefore may depend on the cellular context of the proliferative signal. *Drosophila* C-terminal SRC kinase, CSK, negatively regulates SRC42A mediated signalling, and SRC42a has been demonstrated to signal through JNK and JAK/STAT pathways to promote proliferation, and through the JAK/STAT pathway to trigger apoptosis (Laberge et al., 2005). Whilst it is cleat that SRC42A plays a role in the regulation of cell proliferation, its precise role in these pathways remains to be determined.

Exactly how halving the dose of *src42A* functions to suppress the GMR>DRAD21$^{DM}$ phenotype remains to be seen. However, if SRC42A is functioning as a negative regulator of the MAPK cascade, it would be predicted that halving the dose of *src42A* would result in an upregulation of MAPK response genes. Therefore, halving the dose of *src42A* should behave similarly to the activated form of RAS (sev-RAS$^{V12}$), which constitutively transduces a signal, and therefore results in upregulation of MAPK response genes. Expression of sev-RAS$^{V12}$ in the developing eye in combination with GMR>DRAD21$^{DM}$ results in a dominant enhancement of the small and rough eye phenotype (Figure 5.24). This is opposite to the phenotype observed when the dose of *src42A* is halved and suggests that SRC42A is not functioning as a negative regulator of the MAPK signal in the posterior differentiating cells of the eye imaginal disc, and is most likely functioning as a positive regulator of proliferation. If SRC42A is functioning as a positive regulator of cell proliferation it could be envisaged that slowing the progression of the cell cycle could allow greater time to resolve sister chromatid cohesion and therefore suppress the GMR>DRAD21$^{DM}$ phenotype.

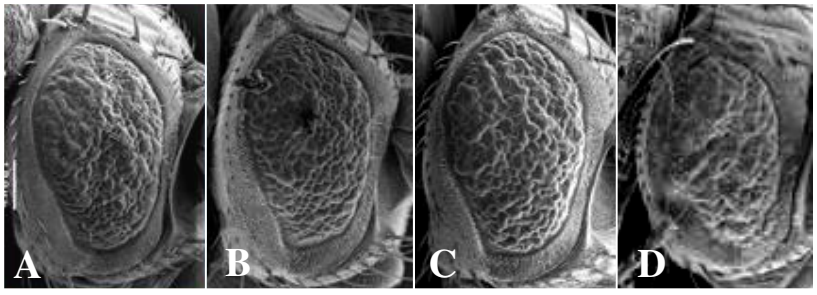


**Figure 5. 24:** *Src42A is likely to function as a positive regulator of cell division in the Drosophila eye*

Scanning electron micrographs of adult *Drosophila* eyes, dorsal side is up and anterior to the right. **A:** The reduced and roughened eye phenotype of GMR>DRAD21$^{DM}$. **B** and **C:** The size and organisation defects of the GMR>DRAD21$^{DM}$ phenotype are mildly suppressed by the *Src42A* alleles *Src42A$^{E1}$* and *Src42A$^{myri}$*. **D:** The organisation and size defects of the GMR>DRAD21$^{DM}$ phenotype are moderately enhanced by the expression of activated RAS in the developing eye (sev-RAs$^{V12}$).

### 5.2.11 COMPLEX GENETIC INTERACTIONS IN CYTOLOGICAL REGIONS 26, 27 AND 28 OF CHROMOSOME 2L

#### 5.2.11.1 Region overview

The genome-wide screen (Section 4.2.2) identified a total of five deficiencies within polytene divisions 26, 27 and 28 that were capable of modifying the GMR>DRAD21$^{DM}$ phenotype. Deficiencies Df(2L)BSC7, Df(2L)XE-3801 and Df(2L)BSC41 enhanced the reduced and roughened GMR>DRAD21$^{DM}$ eye, whilst deficiencies Df(2L)Spd$^{j2}$ and Df(2L)Dwee1-W05 suppressed the GMR>DRAD21$^{DM}$ eye phenotype (Figure 5.25).

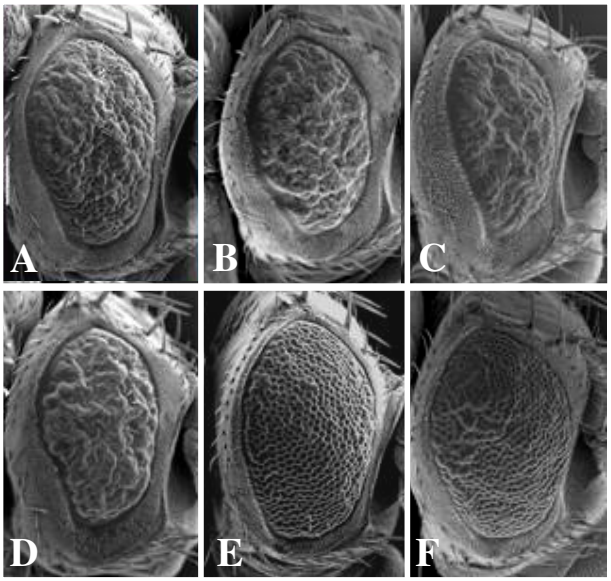


**Figure 5. 25:** *The GMR>DRAD21$^{DM}$ phenotype is enhanced and suppressed by deletions in region 26-28 of chromosome 2L*

Scanning electron micrographs of adult *Drosophila* eyes, dorsal side is up and anterior to the right. A: The reduced and roughened eye phenotype of GMR>DRAD21$^{DM}$. B: The GMR>DRAD21$^{DM}$ phenotype is enhanced by the introduction of Df(2L)BSC7 (E94). C and D: The size and organisation defects of the GMR>DRAD21$^{DM}$ phenotype are also enhanced by the deficiencies Df(2L)XE-3801 (E151) and Df(2L)BSC41 (E100) respectively. E: The GMR>DRAD21$^{DM}$ size and organisation defects are strongly suppressed by Df(2L)Spd$^{j2}$ (S103). F: The Df(2L)Dwee1-W05 deficiency strongly suppresses the size and organisation defects of the GMR>DRAD21$^{DM}$ phenotype, and also exhibits a slight but distinct associated overgrowth phenotype (S48).

#### 5.2.11.2 Genetic dissection of region

In order to further dissect the interactions occurring in this region a significant number of overlapping and internal deletions were obtained and tested. Two additional Deficiency Kit deletions have breakpoints that fall within this region of the genome, neither of which modify the GMR>DRAD21$^{DM}$ eye phenotype. The first of these, Df(2L)BSC6 the breakpoints 26D3-E1;26F4-7, and the second deficiency, Df(2L)Trf-C6R31, has the imprecisely defined breakpoints 28DE. These deletions flank the entire region of interest and therefore aid minimally in clarifying the precise regions responsible for the observed enhancement and suppression. Df(2L)BSC41 has the breakpoints 26D-E;28C and therefore spans almost the entire polytene divisions 26, 27 and 28. Df(2L)BSC41 strongly suppresses both the organisation and size defects of the GMR>DRAD21$^{DM}$ eye phenotype (data not shown ), suggesting that the suppressor interactions within this region are stronger than the enhancer interactions. An additional deficiency, Df(2L)J-H, was obtained and tested. This deficiency has the breakpoints 27C2-9;28B3-4, deleting a smaller region than that of Df(2L)BSC41. This deficiency also suppresses the GMR>DRAD21$^{DM}$ eye phenotype. Two additional deletions that do not modify the GMR>DRAD21$^{DM}$ eye phenotype fall within the region deleted in Df(2L)J-H. These deletions are named Df(2L)ade3 and Df(2L)DE and have the breakpoints 27D1-2;27F1-2 and 27E1-2;28A1-2 respectively.

Using the data from these overlapping deletions, the interacting regions were narrowed down significantly (Figure 5.26). It is likely that the overall interactions observed in this region are due to at least two individual and separable suppressor loci and at least two individual and distinct enhancer loci (Figure 5.26).

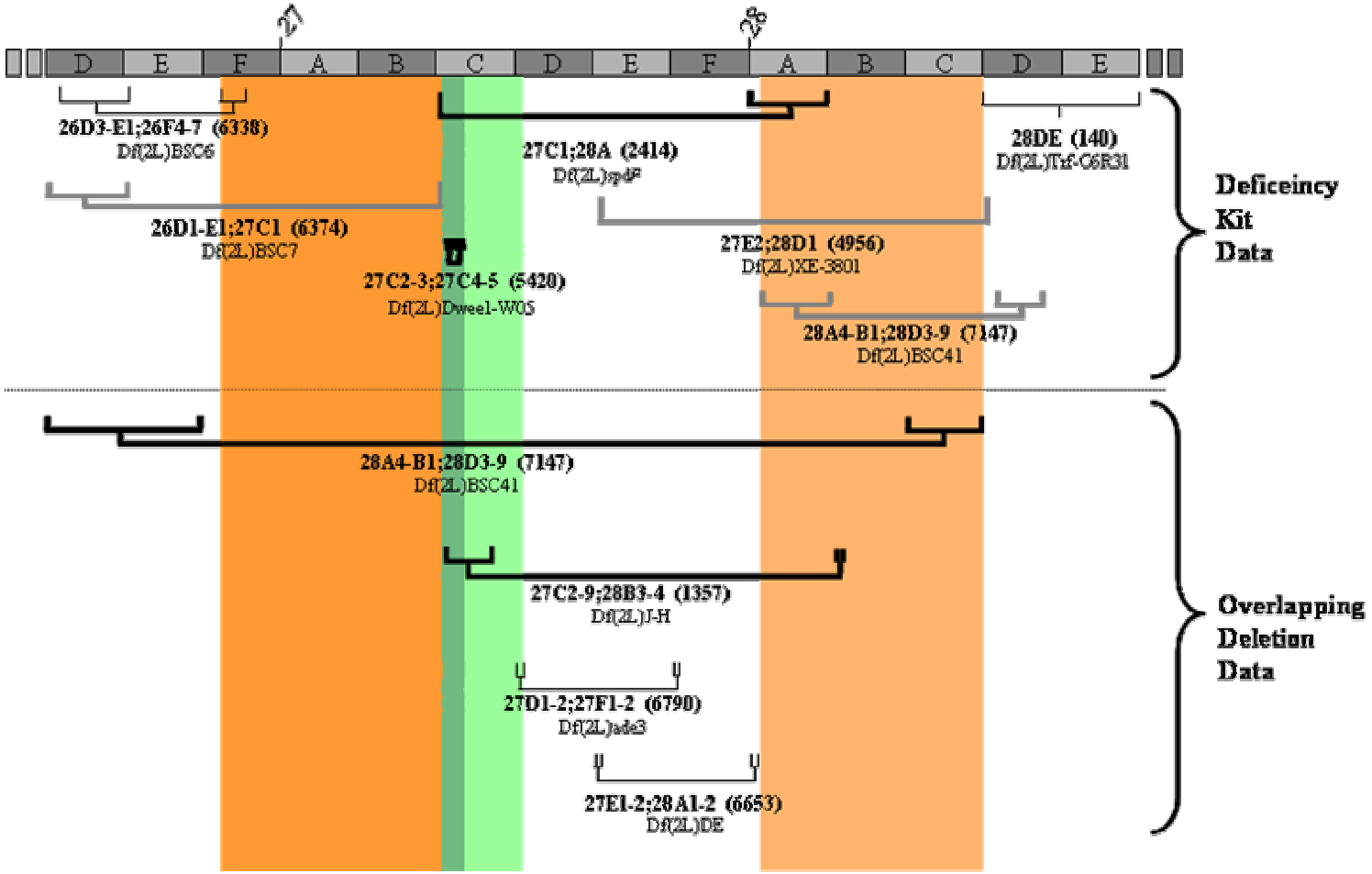
27
28
D E F A B C D E F A B C D E
26D3-E1;26F4-7 (6338)
Df(2L)BSC6
26D1-E1;27C1 (6374)
Df(2L)BSC7
27C2-3;27C4-5 (5420)
Df(2L)Dwee1-W05
27C1;28A (2414)
Df(2L)spd2
27E2;28D1 (4956)
Df(2L)XE-3801
28DE (140)
Df(2L)Tsf-C6R31
28A4-B1;28D3-9 (7147)
Df(2L)BSC41
Deficeincy Kit Data
28A4-B1;28D3-9 (7147)
Df(2L)BSC41
27C2-9;28B3-4 (1357)
Df(2L)J-H
27D1-2;27F1-2 (6790)
Df(2L)ade3
27E1-2;28A1-2 (6653)
Df(2L)DE
Overlapping Deletion Data

**Figure 5. 26:** *Schematic of the complex genetic interactions in polytene divisions 26, 27 and 28*

Polytene divisions 26, 27 and 28 of chromosome 2R are indicated and sub-divisions within are shown. Deletions that suppress the GMR>DRAD21$^{DM}$ eye phenotype are indicated by thick black lines Deletions that enhance the GMR>DRAD21$^{DM}$ eye phenotype are indicated by thick grey lines. Deletions that do not modify GMR>DRAD21$^{DM}$ are indicated by thin black lines. Breakpoints and deficiency names are shown under each deletion, as are the Bloomington stock numbers (brackets). Breakpoints are mapped cytologically and in many cases are estimates only. All deletions shown above the dotted line comprise part of the Deficiency Kit. The narrowed regions likely to contain suppressor loci are indicated by the green blocks, and the narrowed regions likely to contain enhancer loci are indicated by orange blocks.

### 5.2.11.3 Suppressor regions 27C2-3; 27C4-5 and 27C4-5;27D1-2.

Deficiency Df(2L)Dwee-W05, responsible for S48, is completely spanned by that of S103 (Df(2L)spd$^{j2}$). S103 and S48 strongly suppress the GMR>DRAD21$^{DM}$ reduced and disorganised phenotype, however S48 has an additional associated overgrowth phenotype (Figure 5.25). These phenotypic data indicate that the S103 interaction is not solely due to a locus that is common to the two deletions and that there must exist at least two suppressor loci within the region of the Df(2L)spd$^{j2}$ deletion. Using the data obtained from testing overlapping deficiencies the suppressor regions were genetically defined as 27C2-3;27C4-5 and 27C4-5;27D1-2.

The suppressor region responsible for S48 (27C2-3;27C4-5) deletes a maximum of four polytene bands and nine genes. Analysis of the annotations of the genes in this region reveals one obvious candidate gene, *wee*, however given the small number of genes in this region alleles for *Hrb27C, l(2)k0922* and *x16* were also obtained and tested. *x16* encodes a product with mRNA processing activity thought to be a component of the spliceasome (Drysdale et al., 2005) and is expressed in the eye-antennal disc during larval development. The *x16*$^{k00230}$ insertion allele did not modify the GMR>DRAD21$^{DM}$ phenotype. *l(2)k0992* encodes an essential protein with unknown function. The insertion allele *l(2)k0992*$^{k0992}$ did not modify the GMR>DRAD21$^{DM}$ eye phenotype. *wee* encodes a CDC2 inhibitory kinase required to prevent the premature activation of mitosis and for maintaining the integrity of the mitotic spindle (Price et al., 2000, Price et al., 2002, Stumpff et al., 2004, Stumpff et

al., 2005). Neither the *wee*$^{DS1}$ hypomorphic allele nor the *wee*$^{ES1}$ amorphic truncation were able to modify the GMR>DRAD21$^{DM}$ phenotype.

*Hrb27C*, located at 27C4, encodes a heterogeneous nuclear ribonucleoprotein with known roles in RNA splicing and of dorsal-ventral axis positioning during oogenesis through control of RNA localisation (Siebel et al., 1992, Goodrich et al., 2004). The insertion alleles *Hrb27C*$^{02647}$ and *Hrb27C*$^{k02814}$ are both capable of suppressing the size and organisation defects of the GMR>DRAD21$^{DM}$ phenotype (Figure 5.27). These results indicate that deletion of *Hrb27C* is primarily responsible for the S48 interaction and at least in part responsible of the S103 interaction.

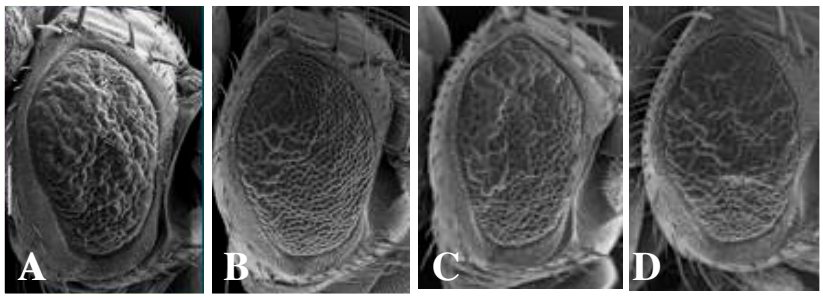


**Figure 5. 27:** *Two different Hrb27C alleles suppress the GMR>DRAD21$^{DM}$ eye phenotype*
Scanning electron micrographs of adult *Drosophila* eyes, dorsal side is up and anterior to the right. **A:** The reduced and roughened eye phenotype of GMR>DRAD21$^{DM}$. **B:** The GMR>DRAD21$^{DM}$ phenotype is suppressed by the introduction of Df(2L)Dwee-W05 (S48). **C** and **D:** The size and organisation defects of the GMR>DRAD21$^{DM}$ phenotype are also suppressed by the *Hrb27C* alleles, *Hrb27C*$^{02647}$ and *Hrb27C*$^{k02814}$ respectively.

The additional suppressor region responsible for S103 spans polytene regions 27C4-5;27D1-2. There are only ten genes that map to this location and analysis of their annotations reveals the cohesin component, *SA* (also referred to as *Scc3*) and the *Drosophila* SUMO-1 orthologue, *smt3*, as candidate genes in this region.

*SA* encodes the *Drosophila* homologue of the SCC3 cohesin subunit and is located at 27C7. Preliminary analysis of GMR>DRAD21$^{DM}$ genetic interactions (Section 4.2.1) showed that, consistent with the Deficiency Kit screen results, deleting the genomic region containing *SA* strongly suppressed the GMR>DRAD21$^{DM}$ eye phenotype, whilst duplication of the region strongly enhanced the phenotype. In the absence of any *SA*mutations the contribution of deleting *SA* alone to the S103

phenotype is unable to be assessed at this point. One way to assess whether the S103 phenotype is primarily due to deletion of *SA* would be to introduce a wild-type *SA* transgene, with its endogenous promoter, into the Df(2L)Spd$^{j2}$ deletion background and test whether this abrogates any interaction with GMR>DRAD21$^{DM}$. If the S103 interaction is primarily due to deletion of *SA* the re-introduction of wild-type levels of SA should abolish any genetic interaction.

*smt3* encodes the *Drosophila* orthologue of the yeast SUMO-1 protein which is involved in protein modification and implicated in regulation of cohesin dissociation in both budding and fission yeast (Stead et al., 2003, Tanaka et al., 1999a, Bachant et al., 2002). The *smc3*$^{04493}$ insertion allele was obtained and shown to be capable of suppressing the size but not the organisation defect of the GMR>DRAD21$^{DM}$ eye phenotype (Figure 5.28), indicating that the S103 interaction is due, at least in part to deletion of *smt3*.

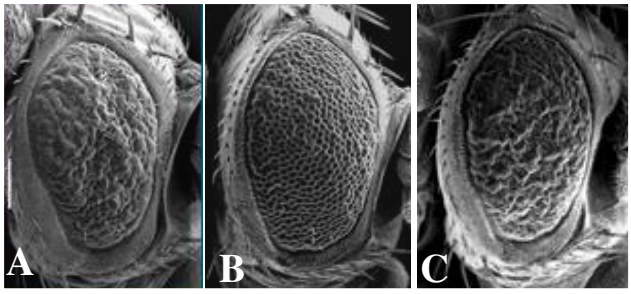


**Figure 5. 28:** *The smt3*$^{04493}$ *insertion allele suppresses the GMR>DRAD21*$^{DM}$ *size defect*

Scanning electron micrographs of adult *Drosophila* eyes, dorsal side is up and anterior to the right. **A:** The reduced and roughened eye phenotype of GMR>DRAD21$^{DM}$. **B:** The GMR>DRAD21$^{DM}$ phenotype is suppressed by the introduction of Df(2L)Spd$^{j2}$ (S103). **C:** The size but not the organisation defects of the GMR>DRAD21$^{DM}$ phenotype are also suppressed by the *smt3*$^{04493}$ insertion allele.

#### 5.2.11.4 Enhancer regions 26F4;27C1 and 28A4;28D1

Df(2L)BSC6 does not modify the GMR>DRAD21$^{DM}$ phenotype and its breakpoints allowed the enhancer region responsible for E94 (Df(2L)BSC7) to be narrowed to 26F4;27C1. This region contains 33 genes and careful analysis of their annotations revealed a single candidate enhancer locus: *Rca1*.

*Rca1* encodes a protein that functions in regulating mitotic entry and controls the timing of cyclin degradation. Homozygous *Rca1*mutants fail to enter mitosis due to the early degradation of mitotic cyclins by the anaphase promoting complex (APC) (Dong et al., 1997, Grosskortenhaus and Sprenger, 2002). Its role in regulating the timing of cyclin destruction and therefore cell cycle progression makes the *Rca1* locus a candidate for the E94 interaction. Unfortunately *Rca1* alleles, whilst publicly available, were unable to be obtained and tested, and therefore the contribution of this locus to the E94 phenotype remains to be assessed.

The deficiencies responsible for E100 and E151 are Df(2L)BSC41 and Df(2L)XE-3801 respectively. These deletions overlap extensively and modify the GMR>DRAD21$^{DM}$ phenotype to similar extents, strongly enhancing the size and organisation defects (Figure 5.25). It is therefore likely that the interactions observed are due to a single locus or region, defining the interacting interval as most probably being the region common to both deletions, 28A4-B1;28D1. This was confirmed in the second-pass screening for modifiers of apoptosis (Section 4.2.4) where both E100 and E151 were shown to be capable of enhancing the GMRhid small eye phenotype. These results indicate that the enhancement of the GMR>DRAD21$^{DM}$ phenotype is an indirect result of increased levels of apoptosis in both E100 and E151. The data from testing overlapping deletions provides further evidence that the enhancing loci reside in the region common to both Df(2L)BSC41 and Df(2L)XE-3801 (Figure 5.26 pale orange block). Analysis of the annotations of the genes in this region does not reveal any obvious anti-apoptosis candidates, indicating that it is possible that there is a novel anti-apoptotic gene in this region.

#### 5.2.11.5 Proposed mechanism of suppression by *Hrb27C*

HRB27C is an essential protein with roles in RNA splicing, protein stabilisation, transcription and nuclear transport. HRB27C also has been shown to have a role in the regulation of chromosome structure in nurse cells during oogenesis (Dej and Spralding 1999). During oogenesis the chromosomes of the endoreplicating nurse cells are polytene, as oogenesis progresses the chromosomes begin to disperse, a process that is completed by stage six of oogenesis. It is believed that sister-chromatid cohesion is one of the forces that must be overcome in order for dispersal to occur. The mechanism of chromosome dispersal is hypothesised to involve activation of the APC, SECURIN degradation and subsequent activation of SEPARASE and cleavage of the DRAD21 cohesin component (Kashevsky et al., 2002). In *Hrb27C* mutants, nurse cell polytene chromosomes fail to disperse, a phenotype that is also observed in *squid* and *ovarian tumour* mutants (Goodrich et al., 2004). This phenotype implicates *Hrb27C* in the regulation of cohesin dissolution, at least in the context of the nurse cell polytene chromosome.

The conservation of cohesin regulation across species means that it is unlikely that this function of HRB27C is specific to nurse cells. If this function of HRB27C is conserved in other tissues it can be conceived that halving the dose of *Hrb27C* may somewhat delay the activation of SEPARASE and therefore prolong the metaphase to anaphase transition, providing longer time for the connections between the sister chromatids to be resolved.

#### 5.2.11.6 Proposed mechanism of suppression by *smt3*

*smt3* encodes the *Drosophila* orthologue of the yeast SUMO-1 protein, functionally similar to ubiquitin (Stead et al., 2003, Tanaka et al., 1999a, Bachant et al., 2002). The *S. pombe smt3* orthologue, *pmt3*, has functions in regulating centromere proteins involved in chromosome segregation, and *pmt3* mutations result in chromosome segregation defects. Budding yeast *smt3* mutants delay in G2/M phase of the cell cycle and have precociously separated sister centromeres (Li and Hochstrasser, 1999, Li and Hochstrasser, 2000) In budding yeast, the cohesin accessory protein PDS5, required for cohesin maintenance but not establishment (Stead et al., 2003, Tanaka et al., 2001), is sumoylated. It is hypothesised that sumoylation of PDS5 is the first step in promoting the separation of sister chromatids, inducing a conformational change that allows SEPARASE to access the cohesin complex (Stead et al., 2003). Mutations in the budding yeast *smt4* SUMO isopeptidase also have separated sister centromeres in G2/M arrested cells, with no detectable RAD21 cleavage or cohesin dissociation from chromosomes (Bachant et al., 2002). These data implicate sumoylation and the proteins involved in directly regulating sister chromatid segregation in mitosis. If this observed role of sumoylation is conserved in metazoan species it is likely that halving the dose of *smt3* is suppressing the GMR>DRAD21$^{DM}$ phenotype by weakening sister chromatid cohesion in the vicinity of the centromere and therefore counteracting the effects of DRAD21$^{DM}$ expression.

## 5.3 DISCUSSION

### 5.3.1 IDENTIFICATION OF INTERACTING LOCI

A multi-pronged approach (detailed in Section 5.2.1 and Figure 5.1) was used to analyse 10 regions of the genome that were identified as modifying the GMR>DRAD21$^{DM}$ phenotype (section 4.2.2). Overlapping deletions were first used, where possible, to genetically narrow down the size of the interacting region. Analysis of the annotations of the genes within each of the refined intervals allowed the identification of candidate suppressor and enhancer loci. When mutant alleles of candidate interacting loci were available, these were obtained and tested to see if they were able to modify the GMR>DRAD21$^{DM}$ eye phenotype. Using this approach, 10 suppressor and three enhancer loci were unequivocally identified (Table 5.1).

**Table 5. 1:** GMR>DRAD21$^{DM}$ interacting loci identified

| Identifier | Interaction Class | Gene | Observed interaction | Gene Function |
|---|---|---|---|---|
| **S122** | Weak 1 Suppression | ***CyclinA*** | suppression | Cell Cycle |
| **S158, S82** | Strong Suppression | ***Cdk7*** | suppression | Cell Cycle |
| **S164** | Strong Suppression | ***prod*** | suppression | Chromosome condensation |
| **S79** | Weak 3 Suppression | ***hdac4*** | suppression | Histone Modification |
| **S67** | Strong Suppression | ***dup*** | suppression | DNA Replication, cohesin recruitment |
| **S81** | Moderate-Strong Suppression | ***scim13*** | suppression | Chromosome segregation |
| **S107** | Mixed Suppression | ***eIF-4a*** | suppression | Translation |
| **E97** | Strong Enhancement | ***kni*** | enhancement | Segmentation, S-phase |
| **E60** | Strong Enhancement | ***mle*** | enhancement | Dosage Compensation |
| | | ***EcR*** | enhancement | Development |
| | | ***Src42A*** | suppression | Cell Cycle |
| **Cytological divisions 26, 27 and 28** | Range of suppression and enhancement (section 5.2.11) | ***Hrb27C*** | suppression | RNA binding |
| | | ***smt3*** | suppression | Sumoylation |

### 5.3.2 PROS AND CONS OF USING THE DEFICIENCY KIT TO SCREEN THE GENOME

Screening the genome using the Deficiency Kit allows the rapid scanning for interacting regions of the genome. Once interacting regions are identified, efforts towards identifying the causative locus/loci can focus on these genetically defined intervals. This provides a very efficient and effective way to identify loci involved in a given process. However, there are also drawbacks to employing such methods. As illustrated by the complex interactions described in this chapter, conflicting interactions with more than one locus can arise. This was particularly evident in the case of region E60. Whilst the overall deletion of the region enhanced the GMR>DRAD21$^{DM}$ phenotype, subsequent candidate gene analysis indicated that this interaction was due to at least two enhancer loci (*mle* and *EcR*) and one suppressor locus (*Src42A*). These data also highlight the fact that interactions observed through simultaneously halving the dose of numerous genes frequently reveal the sum of the effects of removing more than one interacting locus.

Throughout this study, overlapping deletions and mutations of given chromosomal loci rarely interacted with GMR>DRAD21$^{DM}$ to the same extent as the original deficiency, a phenomenon that has also been described for other genetic screens in *Drosophila* (Greaves et al., 1999). Nevertheless, interacting deficiencies were narrowed down to either one, or a couple, of loci that when mutated interacted significantly themselves.

The screen performed in this study is not exhaustive as the Deficiency Kit used only covers approximately 90% of the genome. In addition, the existence of additional interacting loci within each region cannot be ruled out as the results presented cannot exclude the possibility that opposite interactions within the one deficiency mask each other, or that weaker interactions are masked by stronger interactions. Therefore, the total number of interacting loci identified in this screen is likely to be a slight underestimate of the total encoded in the genome.

### 5.3.3 PROS AND CONS OF USING THE CANDIDATE GENE APPROACH TO IDENTIFY INTERACTING LOCI

The candidate gene approach employed in this study is inherently biased. In many cases the identification of candidate interacting loci depended on the function already prescribed to them in FlyBase. It therefore comes as no surprise that the majority of interacting loci identified at the molecular level, such as *prod* and *dup*, have already been implicated in mitosis and chromosome segregation. Although for many of the genes identified this is the first evidence of such a role in *Drosophila*.

It was not possible to significantly narrow down the region of interaction for some of the identified interacting deficiencies as overlapping deletions were unavailable or the breakpoints uninformative. When this was the case, the candidate gene approach proved extremely useful. An example of this is region S81, in which *Scim13* was identified as a suppressor locus. After analysing the information from neighbouring deficiencies, this narrowed region still contained a minimum of 81 genes, of which *Scim13* was one. Using the candidate gene approach, seven candidate interacting loci were identified, five of which had publicly available alleles and were able to be tested directly. Whilst the contribution of other, untested loci, to the S81 suppression phenotype cannot be ruled out, this example clearly illustrates the usefulness of the candidate gene approach.

In cases where the interacting region was significantly narrowed down, or where few mutant alleles were publicly available, candidate genes were chosen less stringently. This approach allowed the identification of *eIF-4A* as a suppressor locus.
These data suggest that the strategy of significantly narrowing the region of interaction using overlapping deficiencies before employing the candidate gene approach is likely to yield further novel regulators of chromosome segregation.

### 5.3.4 THREE MAIN SUPPRESSION MECHANISMS

Ten individual loci capable of suppressing the GMR>DRAD21$^{DM}$ phenotype were identified (Table 5.1). From this limited data-set it appears that there are three general mechanisms through which GMR>DRAD21$^{DM}$ suppression is occurring. The first of these mechanisms is through chromatin modification, the second is through the regulation of M-phase entry and the third is through direct regulation of chromosome segregation. Each of these mechanisms are discussed with specific examples below.

#### 5.3.4.1 Suppression by histone modification

In metazoan species the cohesin complex is removed from chromosome arms during prophase in a cleavage independent manner that involves the mitotic kinases POLO and AURORA. The remaining centromeric pool of cohesin is proteolytically cleaved by SEPARASE at the metaphase to anaphase transition to allow the separation of sister chromatids (Gimenez-Abian et al., 2004, Waizenegger et al., 2000). Differential regulation of arm and centromeric cohesion is not unique to multicellular eukaryotes, however. Studies in fission yeast have shown that heterochromatin is required for the recruitment and/or stabilisation of cohesin at the centromere (Bernard and Allshire, 2002, Bernard et al., 2001b, Nonaka et al., 2002). This study further supports the importance of the chromatin state in cohesin regulation with *prod*, required for correct centromeric condensation, and *hdac4* involved in histone modification, identified as suppressors of the GMR>DRAD21$^{DM}$ phenotype.

The observation that alleles of *prod* and *hdac4* can modify the GMR>DRAD21$^{DM}$ phenotype suggest it is possible that both PROD and HDAC4 are necessary for the recruitment of cohesin, either globally or specifically in the vicinity of the centromere. If this is so, halving the genetic dose of either *prod* or *hdac4* is likely to decrease the strength of centromeric cohesion, and therefore counter-balance the strengthening effect of DRAD21$^{DM}$ expression, ultimately causing a suppression phenotype.

#### 5.3.4.2 Suppression by M-phase regulation

A key role of the cohesin complex is to ensure the bipolar attachment of microtubules to the centromeres of the sister chromatids (Tanaka et al., 2000) and vertebrate cells depleted of *Rad21*arrest in prometaphase without all chromosomes aligned on the metaphase plate and with an activated spindle checkpoint. Defects in cohesin components that prevent the formation of functional cohesin complexes are, therefore, likely to trigger the spindle checkpoint due to lack of tension across the spindle. In contrast, however, defects in cohesin components that do not interfere with complex formation do not trigger cell cycle arrest. This is exemplified when separase-resistant human RAD21 is overexpressed in cell culture. Cells expressing non-cleavable RAD21 were observed to enter anaphase with sister chromatids that were still attached, resulting in the formation of anaphase bridges and a marked increase in aneuploidy (Hauf et al., 2001). It is therefore likely that cells expressing GMR>DRAD21$^{DM}$ are behaving in the same manner. This supposition is supported by the observation that halving the dose of positive cell cycle regulators such as *CycA, CycB, Cdk7* and *eIF4a* suppress the GMR>DRAD21$^{DM}$ eye phenotype whilst halving the dose of negative cell cycle regulators such as *kni* is observed to enhance the GMR>DRAD21$^{DM}$ phenotype. Halving the dose of positive regulators of M-phase may be acting to slow the rate of M-phase entry or progression. If this is so, suppression of the GMR>DRAD21$^{DM}$ phenotype is likely to be occurring as a direct result of the increase time in mitosis to resolve the connections between the replicated chromosomes, including catenation. In this respect, halving the dose of *CycB, CycA, Cdk7* and *eIF4a* could be seen to be imposing an artificial 'checkpoint-like' state on the cells. Conversely, halving the dose of a negative regulator of M-phase is likely to result in cells having less time to resolve the connections between chromatids and therefore increase the level of chromosome missegregation and ultimately the severity of the GMR>DRAD21$^{DM}$ phenotype.

These results, in combination with cell culture studies of non-cleavable human RAD21, suggest that defects in the dissolution of cohesin, for example impaired RAD21 cleavage, would not result in cell cycle arrest and through persistent chromosomal non-disjunction events may be a cause of genomic instability.

#### 5.3.4.3 Suppression by regulation of sister chromatid separation, or cohesin

The function of the cohesin complex is regulated at several distinct levels including cohesin loading onto chromatin, the establishment of cohesion and the dissolution of sister chromatid cohesion. Loading of cohesin prior to DNA replication requires the function of the SCC2 and SCC4 proteins (Ciosk et al., 2000), whilst establishment of cohesion between the newly replicated chromatids requires the ECO1 protein (Toth et al., 1999). Additional proteins are required for the dissolution of the cohesin complex and therefore chromosome segregation. In metazoa, the mitotic kinases Polo and Aurora are required for SCC3 hyperphosphorylation which triggers the prophase cohesin dissociation pathway (Hauf et al., 2005). Centromeric cohesion is removed following proteolysis of the RAD21 cohesin component by separase, a process that is enhanced by Polo-kinase phosphorylation. Separase is kept inactive until the metaphase to anaphase transition by inhibitory binding by separase and Cdc2 mediated inhibitory phosphorylation (Stemmann et al., 2001). In addition, the cellular localisation of separase is tightly controlled and requires CDC28 mediated phosphorylation (Agarwal and Cohen-Fix, 2002). Although incomplete, this short description of cohesin regulation highlights some of the different levels of cohesin regulation.

Some known regulators of cohesin function were identified in this study as suppressors of the GMR>DRAD21$^{DM}$ phenotype. In assessing whether the GMR>DRAD21$^{DM}$ phenotype was suitable for use in a genetic screen (Section 4.2.1) it was observed that halving the dose of *scc2/nippedB* was capable of suppressing the GMR>DRAD21$^{DM}$ phenotype (Figure 4.2). Consistent with this the *scc2/nippedB* recruitment factor, *dup*, was identified as a suppressor of GMR>DRAD21$^{DM}$ in the genome wide screen (Section 5.2.5, Figure 5.10). These results indicate that the results of this genetic screen are likely to provide insights into the recruitment of cohesin in *Drosophila*. Similarly the identification of *smt3* as a suppressor of GMR>DRAD21$^{DM}$ (Section 5.2.11.5) suggests that sumoylation plays a role in the dissolution of metazoan cohesin similar to that already described for yeast (Stead et al., 2003, Bachant et al., 2002).

These results confirm that identification of the loci responsible for all of the interacting regions identified in the Deficiency Kit screen will yield insight into cohesin regulation in metazoan species.

### 5.3.5 FUTURE DIRECTIONS

Significant progress has been made in the identification of the loci responsible for modifying the GMR>DRAD21$^{DM}$ phenotype. However, it is important to attempt identify the interacting locus/loci for all 48 interacting regions identified. To date, 13 interacting loci have been identified at the molecular level (Table 5.1). Although a relatively small number of interacting loci have been identified, they have allowed the identification of general trends in interacting molecules (Section 5.3.3). As the total number of loci identified at the molecular level is increased further insight will be gained into these general trends of suppression and enhancement. Such trends may be highly informative in regards to the regulation of chromosome segregation and specifically the cohesin complex.

#### 5.3.5.1 Identification of remaining GMR>DRAD21$^{DM}$ modifiers

The approach used in this study to identify interacting loci (Section 5.2.1, Figure 5.1) may not be useful for all interacting regions identified in the genome-wide screen. Overlapping deficiencies may not be available to aid in narrowing down the region of interaction. In addition, it is possible that analysis of the annotations of genes within some of the interacting intervals will not identify any obvious candidate interacting loci. An example of this is S86 which belongs to the Moderate-Strong suppressor class (Figure 4.8, Table 4.4). The deficiency responsible for S86 (Df(3L)XG5) has the breakpoints 71C2-3;72B1-C1. Analysis of the breakpoints of overlapping Deficiency Kit deletions allowed the interacting region to be reduced to the 71E4-5;71F1-4 interval. There are currently no additional deficiencies that would aid in further narrowing down this interval. A total of 19 genes, none of which stand out as obvious candidate interactors, map to this region; 11 of these are described purely by their ability to be induced by ecdysone, and four are known by their genome project (CG) number only. There are publicly available stocks for three of the 19 genes in this region. In order to identify the interacting loci in this genetically defined interval, alternative approaches will need to be employed. Each

of the three available mutant stocks in this region contain P-element insertions. One way to narrow down the region of interaction could involve using one of these P-element insertion alleles to create a set of deletions within the region using imprecise P-element excision. Subsequent analysis of these deletions in the GMR>DRAD21$^{DM}$ background, and determination of the deletion breakpoints should allow the region of interaction to be more precisely defined. Such analysis could significantly reduce the number of potential causative genes, which could then be individually introduced into the deletion background to confirm the identity of the causative gene (see Figure 5.1).

#### 5.3.5.2 Analysis of identified modifiers

Once interacting loci have been identified, the mechanism by which the interaction is occurring needs to be established. Exactly what this would entail will depend on the hypothesised mechanism of interaction. In the case of loci, for example *hdac4*, thought to affect cohesin loading further analysis would involve analysing the chromosomal distribution of cohesin components in wild-type and mutant strains. For each of the interacting loci it will be important to establish the effect of mutation on chromosome segregation and chromosome dynamics in the absence of DRAD21$^{DM}$ expression.

#### 5.3.5.3 Quantitation of interaction phenotypes

One drawback of the current approach used to identify and classify enhancers and suppressors of the GMR>DRAD21$^{DM}$ phenotype is the subjectivity of phenotypic assessment. Therefore it will be important to be able to provide an objective, quantitative measure of GMR>DRAD21$^{DM}$ interaction.

Reducing the ability of sister chromatids to disjoin in anaphase, through expression of GMR>DRAD21$^{DM}$, is likely to produce a proportion of cells with an aneuploid chromosome complement. The level of aneuploidy in cells expressing GMR>DRAD21$^{DM}$ can be measured using Florescence Activated Cell Sorting (FACS) analysis. The introduction of a Gal4 responsive, UAS-GFP construct into the GMR>DRAD21$^{DM}$ background will result in cells expressing both DRAD21$^{DM}$ and GFP in the same cells (GMR>DRAD21$^{DM}$,GFP). Thus, GMR>DRAD21$^{DM}$ cells of the eye imaginal disc will be able to be distinguished by virtue of their green

fluorescence. Dissociation of eye imaginal disc cells from individuals expressing GMR>DRAD21$^{DM}$,GFP and subsequent FACS analysis of both cell size and DNA content (ploidy) will provide a quantitative measure of DRAD21$^{DM}$ chromosome missegregation. A suitable control to use for these analyses would be eye imaginal disc cells from flies expressing GFP in the GMR-gal4 defined pattern. Similarly, levels of suppression and enhancement can be quantified in terms of DNA content (ploidy), cell size and cell number by simply crossing the causative deficiency or allele into the GMR>DRAD21$^{DM}$,GFP background and performing such FACS analysis.

# CHAPTER 6: FINAL DISCUSSION

## 6.1 INTRODUCTION

Chromosome segregation and accurate cell division are central to all facets of biology. Indeed, impaired cell division and incorrect chromosome segregation lead to disastrous outcomes such as cell death, and aneuploidy, a hallmark of many cancers and the most commonly recognised cause of birth defects. The mechanisms of cell division and chromosome dissemination into daughter cells have fascinated biologists for centuries. Understanding the molecular mechanisms of such crucial cellular processes will not only satisfy the innate curiosity of the modern cell biologist, but also contribute to a full working knowledge of the genesis of aneuploidy.

In humans, the premature loss of sister chromatid cohesion has been implicated as the most likely cause of sporadic aneuploidy in oocytes of females of advanced maternal age. The bulk of what we understand about sister chromatid cohesion has come from genetic and biochemical studies in yeast and human cells as well as in *Xenopus* cell free extracts. In order to advance our understanding of the processes involved in chromosome segregation in metazoan species this project aimed to generate a genetically amenable *Drosophila* model of chromosome missegregation, and to subsequently use this model to identify regulators of chromosome segregation. The difficulties of dealing with a multicellular model such as *Drosophila* are readily offset by the wealth of genetic tools available and the genomic similarities to human. Indeed, information gleaned from such genetic studies are likely to be highly informative about human pathogenesis given that over 60% of known human disease genes have a *Drosophila* orthologue and when one considers human genes implicated in cancer this number is increased to almost 70% (Fortini et al., 2000, Bernards and Hariharan, 2001, Rubin et al., 2000). However, as such analyses have been based on sequence similarity and not functional studies; it is likely that the true number of human disease gene orthologues present in *Drosophila* may be higher than these initial estimates. Genetic studies such as the one presented in this thesis confirm *Drosophila* as a suitable model organism in which to elucidate the molecular basis of human diseases.

## 6.2 THIS STUDY

At the commencement of this study it was clear that genetic studies in a metazoan species, such as *Drosophila*, could offer unique insights into how metazoan species regulate the structure and stability of their chromosomes. This thesis describes a series of experimental approaches used with the ultimate aim of identifying novel metazoan regulators of chromosome segregation.

The first step in this process was the generation of a dominant DRAD21 isoform that would allow genetic studies, including a genome-wide screen, to be performed. At the commencement of this study, genetic analyses of *Drosophila* cohesin function had not been conducted due to the lack of mutations in genes encoding cohesin components. During the course of this study, DRAD21 localisation and RNAi depletion studies (Vass et al., 2003, Valdeolmillos et al., 2004, Warren et al., 2000b) indicated that DRAD21 function in *Drosophila* chromosome segregation is analogous to that of RAD21 proteins in other species. Depletion of DRAD21 by RNA interference was observed to cause premature separation of sister chromatids, and DRAD21 was found to physically associate with proteins identified as cohesin components based on their homology to know cohesins in other species (Vass et al., 2003). Analysis of DRAD21 localisation by indirect-immunofluorescence and live imaging of *Drosophila* embryos in combination with the RNAi analysis are consistent with DRAD21 playing a key role in the regulation of sister chromatid cohesion (Warren et al., 2000b, Valdeolmillos et al., 2004). However, no previous attempts identify DRAD21 cleavage fragments had been reported in the literature prove that DRAD21 does indeed perform the same function as RAD21 proteins of other species. In addition, due to the lack of *Drad21* germline previously published studies were unable to take advantage of the wealth of genetic tools available to *Drosophila* researchers.

In an effort to further characterise the role of DRAD21 in sister chromatid cohesion in *Drosophila* a series of analyses of DRAD21 cleavage were undertaken. Chapter 3 describes the identification of the separase cleavage sites in DRAD21 through site-directed mutagenesis. Consistent with studies in other species, expression of separase cleavage resistant forms of DRAD21 are inconsistent with cell survival and

result in increased levels of cell death and when expressed in the developing eye, a rough eye phenotype. This increase in the levels of apoptosis was demonstrated to occur specifically in cells expressing the cleavage resistant forms of DRAD21, irrespective of the tissue type, or developmental stage of expression. In addition, $DRAD21^{DM}$ overexpression was found to cause mitotic arrest or delay, and the severity of the $DRAD21^{DM}$ phenotype directly correlated with both the level of transgene expression and with the mitotic index of cells expressing this DRAD21 isoform. Increasing the number of mitoses in $DRAD21^{DM}$ expressing cells increased the severity of the eye phenotype, whilst slowing progression through mitosis by hemizygosity of *CyclinB* suppressed the phenotype. The results presented in Chapter 3 are consistent with $DRAD21^{DM}$ expression resulting in similar chromosome missegregation events to those observed in human cells expressing cleavage resistant RAD21 (Hauf et al., 2001). Western blot analysis of the DRAD21 proteins isolated from eye imaginal discs expressing DRAD21 isoforms provided the first direct evidence of DRAD21 cleavage, presumably by SEPARASE. Unlike the RAD21 proteins of other species examined to date, results obtained in this study show that DRAD21 is preferentially cleaved at or adjacent to R474, and that only a small percentage of DRAD21 is cleaved at or adjacent to R175.

The generation of this dominantly acting DRAD21 isoform served two main purposes, as presented in this thesis. The first of these is that it allowed the first genetic analysis of DRAD21 and cohesin function in *Drosophila,* as discusses above. The second purpose served by the dominant DRAD21 isoform is that it allowed a genome-wide genetic screen for novel regulators of chromosome segregation to be performed. Chapter 4 firstly describes experiments conducted to determine the suitability of the $GMR>DRAD21^{DM}$ eye phenotype for use in a genetic screen by demonstrating the modification of the eye phenotype by known and predicted cohesin interactors. The $GMR>DRAD21^{DM}$ phenotype was then used to screen the *Drosophila* genome for genetic interactors. This genome wide screen identified 62 individual deficiencies that were capable of enhancing or suppressing the $GMR>DRAD21^{DM}$ phenotype. Subsequent analyses reduced the number of interacting genomic regions to 57. This number of identified interactors is consistent with the results of similar genetic screens in *Drosophila.* Using the expression of EP elements in the developing eye Hariharan and colleagues identified 46 lines,

representing 32 individual loci as potential negative regulators of the cell cycle (section 1.2.3.1) (Tseng and Hariharan, 2002). Additionally, a genetic screen designed to identify genes involved in chromosome inheritance identified 78 loci influencing the meiotic chromosome transmission (Dobie et al., 2001). Therefore, the number of modifier loci encoded in the *Drosophila* genome that when hemizygous alter the GMR>DRAD21$^{DM}$ phenotype is of the same order of magnitude as previously reported genetic screens performed both in the developing *Drosophila* eye and for genes involved in chromosome inheritance.

In an attempt to identify as many of the genetic modifiers of the GMR>DRAD21$^{DM}$ phenotype as possible, a candidate gene approach was taken. As described in Chapter 5 this approach resulted in the identification of 13 interacting loci at the molecular level. The loci unequivocally identified include regulators of mitotic entry or progression (eg *CycA*), loci implicated in cohesin regulation (eg *dupI*) and genes with established roles in histone modification (eg *HDAC4*). Whilst a possible mechanism by which of these loci are acting to suppress or enhance the GMR>DRAD21$^{DM}$ phenotype could be postulated for each, the validity of each model remains to be established. Current data indicates an interesting trend, with some interactors having established roles in chromosome cohesion, while others have as yet undefined roles. It is hoped that continued efforts to identify the remaining loci will identify both novel regulators of chromosome segregation and provide a shortlist of genes that when functionally impaired may incrementally increase the risk of chromosome missegregation and aneuploidy in humans.

## 6.3 FUTURE DIRECTIONS

### 6.3.1 IDENTIFICATION OF OTHER INTERACTING LOCI AT THE MOLECULAR LEVEL

Identifying all of the loci responsible for the phenotypic modification of GMR>DRAD21$^{DM}$ will be particularly challenging. The approach employed in this study, of using overlapping deficiencies to narrow down the region of interaction, was particularly useful when analysing genomic regions in which several obvious candidate genes could be identified. This approach was successfully utilised to identify 13 of the 57 GMR>DRAD21$^{DM}$ interactors at the molecular level. For many of the interacting genomic regions remaining to be genetically dissected, however, there are no overlapping deficiencies readily available that would significantly narrow down the region of interaction. In addition, obvious candidate genes cannot be identified in many of the genetically defined regions of the genome found to modify the GME>DRAD21$^{DM}$ phenotype. In these instances, identification of interacting loci at the molecular level will require a different approach than the one utilised in this study.

An attractive strategy that could be used to identify the remaining interacting loci is that of genome wide EMS mutagenesis followed by meiotic mapping of the mutant loci using single nucleotide polymorphisms, or SNPs. EMS mutagenesis causes nucleotide substitutions which result in missense or nonsense mutations (Lifschytz and Falk, 1968). A pitfall in using EMS mutagenesis in the past has been that while this approach has allowed the isolation of a large number of mutations, the positional cloning of such mutations has been both labour and time intensive. This was in part due to the lack of sufficient markers, both phenotypic and molecular, to provide the level of resolution required for such analyses. The recent development of high resolution SNP markers should allow more rapid identification of mutant loci generated by such chemical mutagenesis approaches (Nairz et al., 2002, Berger et al., 2001).

In the case of mutations in essential genes the approximate chromosomal location of EMS induced mutations can be determined by complementation analysis. Failure of EMS mutations to complement chromosomal deficiencies would place the site of the lesion within the cytologically defined breakpoints of the deficiency, or be indicative

of second site bob-complementation. The location of the EMS induced lesions could be confirmed by meiotic mapping using SNPs. This approach could be used to precisely identify the remaining interacting loci at the molecular level. One major advantage of such an approach is that it provides mutant alleles for additional analyses of the identified interacting loci, which is particularly useful in the case of loci for which mutations have not been described or discovered.

An additional advantage of performing an EMS screen to identify GMR>DRAD21$^{DM}$ interactors is that it may allow for the isolation of more subtle mutations that influence chromosome segregation. An EMS screen may also allow the recovery of *Drad21* mutants, which to date have remained elusive. The recovery of *Drad21* mutants in this manner is likely to depend on the allele generated during the EMS mutagenesis. Over-expression of wild-type DRAD21 in the GMR>DRAD21$^{DM}$ cells has no significant affect on the reduced and roughened eye phenotype (data not shown). However, DRAD21 isoforms with reduced capacity to form a complex with other cohesin components, for example, would be expected to enhance the small and rough GMR>DRAD21$^{DM}$ phenotype by increasing the proportion of DRAD21$^{DM}$ containing cohesin on the chromosomes.

## 6.4 IMPLICATIONS

### 6.4.1 HUMAN DISEASE

Chromosome segregation is such a fundamental process that it is not surprising that defects in its regulation can lead to human disease. The contribution of chromosome missegregation to aneuploidy and the implications for cancer and birth defects was a concept introduced in Chapter 1. Indeed, the modifier loci identified in this study are likely to play important roles in the regulation of genomic stability during cell division. Defects in genes identified as modifiers of GMR>DRAD21$^{DM}$ phenotype are therefore likely to cause defects in chromosome segregation when mutated and therefore are implicated in disease phenotypes such as cancer and birth defects where chromosome missegregation plays a major role. However, defects in the cohesin

complex and its regulation are likely to have much more widely reaching implications.

The importance of the cohesin complex in correct development in metazoan species is highlighted in the recent reports of two developmental syndromes that have been found to be the result of defects in key cohesin regulators. These syndromes are Cornelia de Lange Syndrome and Roberts Syndrome.

Cornelia de Lange Syndrome (CdLS; OMIM 122470) is a dominantly inherited complex disorder that includes characteristic facial features, limb abnormalities and growth and mental retardation. The frequency of this disorder is estimated to be as high as 1 in 10 000 live births (Opitz, 1985). Using different approaches of breakpoint analysis and genome-wide linkage analysis, CdLS was shown to be caused by mutations in *NIPBL*, the human homologue of *Drosophila NippedB* and the yeast *Scc2* cohesin loading factor (Krantz et al., 2004, Tonkin et al., 2004). Interestingly, CdLS cells do not exhibit precocious dissociation of sister chromatids as may be expected if cohesin loading is reduced. The molecular mechanism by which *NIPBL* mutations cause CdLS remain to be determined, but the multi-system nature of this disorder may be partially explained by NIPBL acting as a transcriptional regulator, like *Drosophila* NIPPED B.

Roberts Syndrome (RBS; OMIM 268300) is an autosomal recessive disorder characterised by craniofacial abnormalities, symmetrical reduction of all limbs and loss of centromeric sister chromatid cohesion. RBS syndrome is extremely rare, with only about 100 recorded cases, and has recently been shown to be due to mutations in *ESCO2*, the human homologue of the *Eco1* cohesin establishment factor (Vega et al., 2005). Anti-sense mediated inhibition of several genes known to be involved in chromosome segregation such as that encoding the centromeric protein INCENP is capable of recapitulating the RBS cellular phenotype, suggesting a mechanistic link between these processes and RBS pathogenesis (Musio et al., 2004). Precisely how *ESCO2* mutations cause RBS remains to be determined but are likely to involve other proteins known to be involved in chromosome segregation.

The phenotype of RBS cells suggests that the establishment of cohesion between sister chromatid arms, at least in human cells, does not require the function of *ESCO2*, as chromosome arms do not precociously separate in cells isolated from RBS patients. This could be due to cohesin independent cohesion, for example caused by DNA catenation. Alternatively, functional redundancy may allow for the establishment of cohesin mediated cohesion along chromosome arms. This second explanation is the most plausible, given that there are two human *Eco1* homologues with non-redundant functions (Hou and Zou, 2005).

Given that defects in the loading of cohesin and the establishment of cohesion are responsible for the disease phenotypes of CdLS and RBS it is likely that defects in other cohesin regulators will also manifest as pathological states in humans. The identification of novel regulators of chromosome segregation in this study may identify some of the loci implicated in human disease as regulators of chromosome segregation in *Drosophila*. Loci identified in this study as being capable of modifying the GMR>DRAD21$^{DM}$ may, in the long term, provide diagnostic markers for human diseases where disruption of sister chromatid cohesion and/or aneuploidy are contributing factors.

### 6.4.2 GMR>DRAD21$^{DM}$ AS A MODEL OF MEIOSIS I NON-DISJUNCTION

The majority of human gametic aneuploidy has no obvious cause, with the only established risk factor being maternal age. The maternal age effect is exemplified by the observation that the risk of a trisomic conception rising from approximately 1 in 1500 in a woman of 25 years to approximately 1 in 25 in a woman of 40 years (Hassold and Hunt, 2001). The existence of women with a normal karyotype but with a history of aneuploid conceptuses suggests that there are likely to be genetic factors that increase the chance of aneuploid conceptions (Warburton et al., 2004, Munne et al., 2004), however at present there is no means of identifying individuals at increased risk.

Most incidences of aneuploidy that lead to birth defects can be traced to chromosome segregation errors of maternal origin (>80%), with the majority of these (>60%)

occurring during meiosis I (Hassold and Hunt, 2001). Defects in the amount or location of meiotic crossing over (chiasmata) has been linked to meiotic non-disjunction (Revenkova et al., 2001). In mouse knockout studies elevated non-disjunction has been shown to result from a defects in cohesin components REC8 and SMC1β (Revenkova et al., 2004, Xu et al., 2005). These studies have lead to the proposal that premature loss of sister chromatid cohesion is the most likely molecular cause of the maternal age effect.

The implication of cohesins in the maternal age effect is justified when one considers that the sites of meiotic chromosome crossing over are established during foetal development, decades before the chiasmata are resolved just prior to ovulation. It is conceivable that defects in cohesin (that lead also to defects in recombination) could result in the gradual loss of sister chromatid cohesion over time. Indeed, in mice lacking the meiotic SMC1 isoform, SMC1β, a striking age dependent decrease in the percentage of synapsed homologous chromosomes is observed, even though the maternal age effect in mice is modest compared to that of humans (Hodges et al., 2005). These data provide strong support for the hypothesis that defective cohesin is the underlying cause age-related aneuploidy.

Given that sister chromatid arm cohesion is maintained by RAD21-containing cohesin complexes during meiosis I (Klein et al., 1999), the somatic GMR>DRAD21$^{DM}$ phenotype is a reasonable *Drosophila* model of meiosis I non-disjunction. As many of the genes required for the maintenance of genomic integrity are common to both mitosis and meiosis (Gatti et al., 1980, Baker et al., 1978), a somatic assay is likely to yield important information about chromosome segregation events and the molecular players involved in meiosis. Therefore, genetic interactions identified in this study are likely to provide insight into the genetic basis of aneuploidy in both somatic cells and in the germline.

It appears that chromosome segregation provides a classic example of the conundrum that the more you know about a process the more you realise that you don't know, or the more you realise there is to discover. The genetic screen performed in this study has so far implicated 13 genes in the regulation of the structure and stability of metazoan chromosomes during meiotic and somatic cell division. These loci are

known to be involved in such diverse cellular processes ranging from the response to developmental hormone signals, DNA replication and RNA binding. In addition, it is likely that as further genetic modifier loci are identified at the molecular level this list will continue to diversify. Despite the broad range of molecules identified in this study as regulating chromosome segregation, general trends were observed (Section 5.3.3). It will not be until each of these genes are examined in detail and the means by which they influence chromosome segregation determined that we will begin to understand the way in which they combine to regulate the dissemination of the genome into daughter cells.

## 6.5 FINAL COMMENTS

The problem of how a cell divides continues to fascinate cell biologists. Although we now know the identity of many of the molecules involved in the regulation of cell division this knowledge has raised a whole host of new questions. What molecules control the cohesin complex in metazoan species? How is it that certain people have an increased risk of an aneuploid conception? What gives rise to seemingly spontaneous aneuploidy? This thesis describes one approach used to address these questions, and the results of this study will be important for dissecting the molecular mechanism of aneuploidy. Genes identified in this study may, when functionally impaired, incrementally increase the risk of chromosome missegregation and aneuploidy in humans and perhaps, in time, sporadic human aneuploidy will be considered a collection of low penetrance maternal effect conditions. No doubt the data gathered in this and future studies designed to address these questions will give rise to a whole new set of problems that will continue to fascinate biologists for decades, if not centuries to come.